Last Glacial Maximum and Younger Dryas piedmont glaciations in Blidinje, the Dinaric Mountains (Bosnia and Herzegovina)

Çiner, Attila; Stepišnik, Uroš; Sarıkaya, M. Akif; Zebre, Manja; Yıldırım, Cengiz

Published in:
Mediterranean Geoscience Reviews

DOI:
10.1007/s42990-019-0003-4

Publication date:
2019

Citation for published version (APA):
Çiner, A., Stepišnik, U., Sarıkaya, M. A., Zebre, M., & Yıldırım, C. (2019). Last Glacial Maximum and Younger Dryas piedmont glaciations in Blidinje, the Dinaric Mountains (Bosnia and Herzegovina): insights from 36Cl cosmogenic dating. *Mediterranean Geoscience Reviews*, *1*(1), 25-43. https://doi.org/10.1007/s42990-019-0003-4

Mediterranean Geoscience Reviews

Last Glacial Maximum and Younger Dryas piedmont glaciations in Blidinje, the Dinaric Mountains (Bosnia and Herzegovina); insights from 36Cl cosmogenic dating

--Manuscript Draft--

Manuscript Number:	MEGR-D-19-00003R1
Full Title:	Last Glacial Maximum and Younger Dryas piedmont glaciations in Blidinje, the Dinaric Mountains (Bosnia and Herzegovina); insights from 36Cl cosmogenic dating
Article Type:	Original Paper
Funding Information:	TUBİTAK (118Y052) — Dr Mehmet Akif Sarıkaya Bilimsel Araştirma Projeleri Birimi, Istanbul Üniversitesi (MGA-2017-40540) — Dr Mehmet Akif Sarıkaya Slovenian Research Agency (No. P1-0011, No. P6-0229(A) and P1-0025) — Dr Manja Žebre University of Ljubljana — Dr Uros Stepišnik
Abstract:	The highest parts of the Dinaric Mountains along the eastern Adriatic coast of the southern Europe, known for their typical Mediterranean karst–dominated landscape and very humid climate, were glaciated during the Late Pleistocene. Palaeo–piedmont type glaciers that originated from Čvrsnica Mountain (2226 m a.s.l.; above sea level) in Bosnia and Herzegovina deposited hummocky, lateral and terminal moraines into the Blidinje Polje. Twelve boulder samples collected from these moraines were dated by cosmogenic 36Cl surface exposure dating method. Using 40 mm ka–1 bedrock erosion rate due to high precipitation rates, we obtained 36Cl ages of Last Glacial Maximum (LGM; 22.7 ± 3.8 ka) from the hummocky moraines, and Younger Dryas (13.2 ± 1.8 ka) from the lateral moraine in Svinjača area. The amphitheater shaped terminal moraine in Glavice area also yielded a Younger Dryas (13.5 ± 1.8 ka) age within the error margins. Because our boulder ages reflect complex exhumation and denudation histories, future work is needed to better understand these processes and their influence on the cosmogenic exposure dating approach in a karstic landscape. Our results provide a new dataset, and present a relevant contribution towards a better understanding of the glacial chronologies of the Dinaric Mountains.
Corresponding Author:	Attila Çiner, PhD Istanbul Teknik Universitesi Istanbul, TURKEY
Corresponding Author Secondary Information:	
Corresponding Author's Institution:	Istanbul Teknik Universitesi
Corresponding Author's Secondary Institution:	
First Author:	Attila Çiner, PhD
First Author Secondary Information:	
Order of Authors:	Attila Çiner, PhD Uros Stepišnik, Dr Mehmet Akif Sarıkaya, Professor Manja Žebre, Dr Cengiz Yıldırım, Dr
Order of Authors Secondary Information:	
Author Comments:	I have made all requested chages that were pointed out by the reviewers.

Response to Reviewers:	I have made all changes that were pointed out by the referees. As they were minor changes I do not include a rebuttal to reviewers letter here.

Highlights

- Extents of piedmont palaeoglaciers were reconstructed in Bosnia and Herzegovina
- Last Glacial Maximum (LGM) moraine age reported from the Dinaric Mountains
- 5 boulders from hummocky moraines yielded ^{36}Cl ages of 22.7 ± 3.8 ka (LGM)
- 3 boulders from a lateral moraine gave ^{36}Cl ages of 13.2 ± 1.8 ka (Younger Dryas)
- 4 boulders from a terminal moraine gave ^{36}Cl ages of 13.5 ± 1.8 ka (Younger Dryas)
- Boulder ages reflect complex exhumation and denudation histories

Last Glacial Maximum and Younger Dryas piedmont glaciations in Blidinje, the Dinaric Mountains (Bosnia and Herzegovina); insights from ^{36}Cl cosmogenic dating

[a]Attila ÇİNER, [b]Uroš STEPIŠNIK, [a]M. Akif SARIKAYA, [c]Manja ŽEBRE, [a]Cengiz YILDIRIM

[a]Eurasia Institute of Earth Sciences, Istanbul Technical University, Maslak–Istanbul 34469, Turkey

[b]Department of Geography, Faculty of Arts, University of Ljubljana, Aškerčeva 2, 1000 Ljubljana, Slovenia

[c]Department of Geography and Earth Sciences, Aberystwyth University, United Kingdom

Corresponding author: Attila Çiner; cinert@itu.edu.tr

Abstract

The highest parts of the Dinaric Mountains along the eastern Adriatic coast of the southern Europe, known for their typical Mediterranean karst–dominated landscape and very humid climate, were glaciated during the Late Pleistocene. Palaeo–piedmont type glaciers that originated from Čvrsnica Mountain (2226 m a.s.l.; above sea level) in Bosnia and Herzegovina deposited hummocky, lateral and terminal moraines into the Blidinje Polje. Twelve boulder samples collected from these moraines were dated by cosmogenic ^{36}Cl surface exposure dating method. Using 40 mm ka^{-1} bedrock erosion rate due to high precipitation rates, we obtained ^{36}Cl ages of Last Glacial Maximum (LGM; 22.7 ± 3.8 ka) from the hummocky moraines, and Younger Dryas (13.2 ± 1.8 ka) from the lateral moraine in Svinjača area. The amphitheater shaped terminal moraine in Glavice area also yielded a Younger Dryas (13.5 ± 1.8 ka) age within the error margins. Because our boulder ages reflect complex exhumation and denudation histories, future work is needed to better understand these processes and their influence on the cosmogenic exposure dating approach in a karstic landscape. Our results provide a new dataset, and present a relevant contribution towards a better understanding of the glacial chronologies of the Dinaric Mountains.

Keywords: Dinaric Karst; Cosmogenic Surface Exposure Dating; Piedmont Glaciation; Bosnia and Herzegovina; Balkans; Last Glacial Maximum, Younger Dryas

1. Introduction

The Dinaric Mountains extend along the eastern Adriatic coast for about 650 km along the western Balkan Peninsula, from the Alps in Slovenia to the Korab Mountains in Albania and is highly influenced by the Mediterranean climate. Western part of the mountain range is a karst landscape with high–elevated plateaux, which characterise highest segments of the

Dinaric Mountains with elevations reaching 2522 m a.s.l. (above sea level) in Durmitor and 2694 m a.s.l. in Prokletije mountains, where small glaciers still exist (Gachev et al., 2016). The Dinaric Mountains were also glaciated in the past. First studies related to the glaciations of the Dinaric Mountains were carried out in Bosnia and Herzegovina and Montenegro (e.g. Cvijić, 1899; Grund, 1902, 1910; Penck, 1900; Liedtke, 1962; Riđanović, 1966). Pleistocene glaciers were reported from the coastal Dinaric Mountains bordering the Adriatic Sea (Cvijić, 1899, 1900). Because of likely high moisture supply during cold periods (e.g. Hughes et al., 2010), moraines were encountered below 1000 m a.s.l., and glacial deposits were described even at sea level in northern Dalmatia (Croatia) (Marjanac and Marjanac, 2004). Sawicki (1911) reported moraines on Mount Orjen (1894 m) in Montenegro, ~500 m a.s.l., overlooking present level of the Adriatic Sea. Although wars and political instabilities during the last century prevented further research in the countries surrounding the Dinaric Mountains, there is now an increasing interest in the description and understanding of past glacial deposits and events (e.g. Hughes et al., 2010, 2011; Petrović, 2014; Krklec et al., 2015). For instance, the Late Pleistocene glacial landforms and glaciokarst of Mount Orjen were described in detail (Marković, 1973; Stepišnik et al., 2009). Ice caps and valley glaciers also developed elsewhere in the Dinaric Mountains, e.g. in the mountains of Albania (e.g. Milivojević, 2007; Milojević et al., 2008), Montenegro (e.g. Hughes et al., 2011), and Slovenia (e.g. Žebre and Stepišnik, 2015a; Žebre et al., 2016).

Recent interest is focussed on the dating of glacial landforms and their palaeoclimatic interpretations. Although the U–series method lacks the precision needed to constrain the timing of moraine deposition, it can nevertheless bracket moraines within certain glacial cycles, where a first attempt was made on Mount Orjen (Hughes et al., 2010). By dating secondary cements within moraines and outwash fans, Middle Pleistocene (MIS 12; 480–430 ka), and later MIS 6 (190–130 ka) and MIS 5d–2 (110–11.7 ka) glaciations were reported by

Hughes et al. (2010). Cosmogenic ^{36}Cl surface exposure dating is now a well–established method for dating moraines (Dunai, 2010; Gosse and Phillips, 2001), and became a standard tool in dating especially carbonate lithologies and carbonate–derived sediments (e.g. Gromig et al., 2018; Pope et al., 2015; Sarıkaya et al., 2014; Styllas et al., 2018). However, karst denudation rates in extremely moist climatic settings, such as in southwestern Bosnia and Herzegovina, where this study is carried out, limit the confidence in the ^{36}Cl exposure dating technique to rocks older than ~40 ka (Hughes and Woodward, 2017; Levenson et al., 2017 and references therein). A recent study in Bosnia and Herzegovina by Žebre et al. (2019) succesfully tackled this challenging problem and obtained first ^{36}Cl ages from the Dinaric Mountains. A total of 20 moraine boulders yielded ages spanning from Oldest Dryas in Velež Mountain (14.9 ± 1.1 ka) to Younger Dryas in Crvanj Mountain (11.9 ± 0.9 ka) (Žebre et al., 2019).

This paper focuses on the glacial chronology of the Blidinje area in Bosnia and Herzegovina. We therefore aim (a) to overview the geomorphological evidence for glaciation in the Blidinje area, (b) to constrain the timing of the largest recognized glacier extent on Svinjača and Glavice piedmont glaciers by applying the cosmogenic ^{36}Cl surface exposure dating method on lateral, terminal and hummocky moraines, (c) to discuss the formation of hummocky moraines in a karstic landscape, and (d) to compare the existent chronology with the sourrounding mountains in the Dinaric Mountains and also in wider Balkan Peninsula.

2. Regional setting

The Blidinje area (43° 40'–43° 35' N and 17° 25'–17° 40' E) is located in the central Dinaric Mountains in southern Bosnia and Herzegovina. The central lowered relief, known as Blidinje Polje (Blidinjsko Polje or Dugo Polje), was recently mapped and described by Stepišnik et al. (2016). Blidinje Polje is a southwest–northeast elongated polje ~20 km long and 2–5 km wide, surrounded by Vran Mountain (2074 m a.s.l.) to the northwest, and by Čvrsnica

Mountain (2226 m a.s.l.) to the southeast. The study area is part of Bosnia and Herzegovina high karst (Buljan et al., 2005), mainly composed of more or less permeable Cretaceous and Jurassic carbonate rocks and their Quaternary re–depositions (Sofilj and Živanović, 1979); Stepišnik et al., 2016).

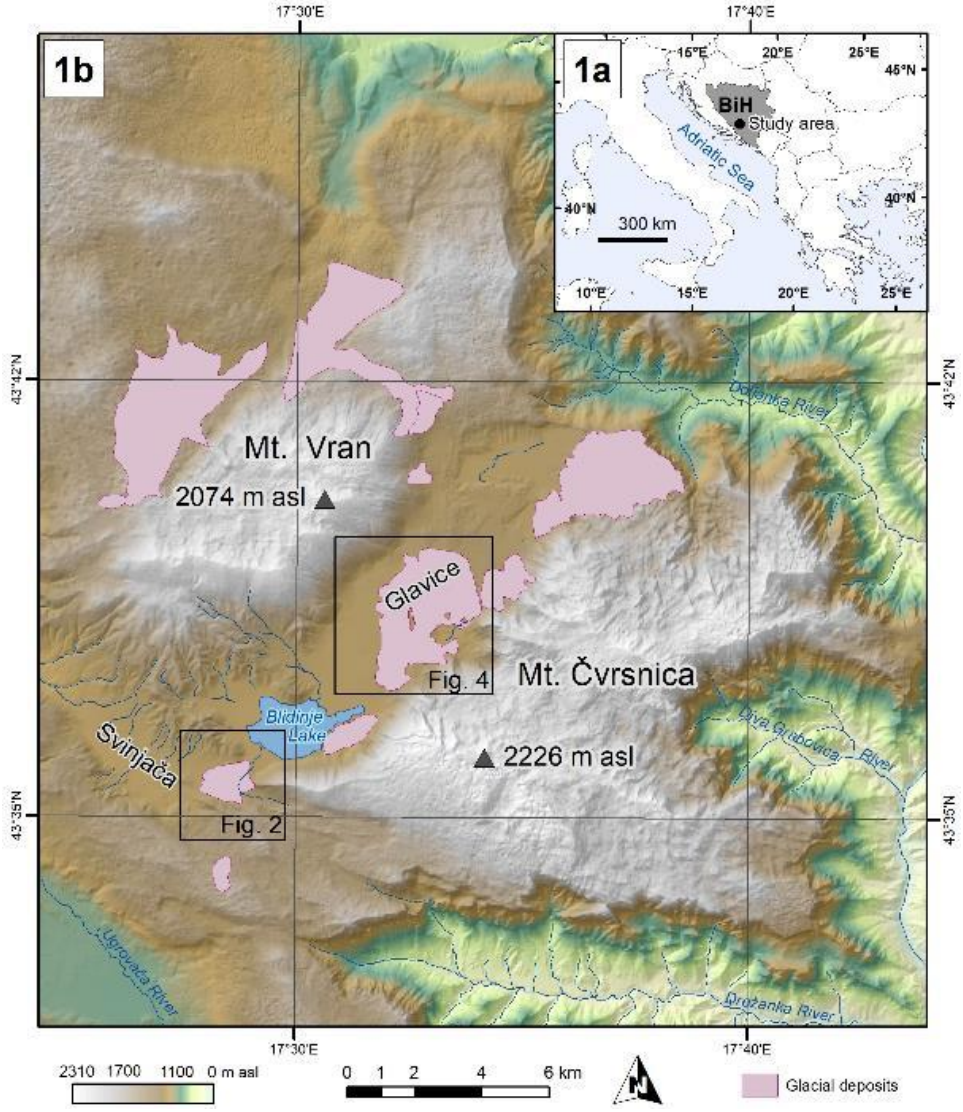

Figure 1: a) Study area location map in Bosnia and Herzegovina (BIH); b) Glacial deposits of Svinjača (Figure 2) and Glavice (Figure 4) are located within the Blidinje Polje. Location of glacial deposits after Stepišnik et al. (2016) and Sofilj and Živanović (1979).

According to the Köppen–Geiger climate classification (Kottek et al., 2006) the study area has characteristics of a warm temperate climate, fully humid, with cool summers (Cfc). The Blidinje area is located within a transition zone between the Mediterranean and continental climate. Precipitation is distributed throughout the year due to the moisture originating from the Adriatic Sea towards west as well as due to orographic precipitation effect. The closest comparable meteorological station is in Nevesinje (891 m a.s.l.), located ~40 km southeast, where mean annual precipitation over the period 1961–1990 was 1795 mm, while the mean annual air temperature for the same 30–year period was 8.6 °C (Data courtesy Federal Hydrometeorological Institute, Sarajevo). Precipitation amount at higher altitudes, such as the Blidinje area and surrounding mountains, is expected to reach more than 2000 mm per year (Vojnogeografski institut, 1969).

3. Methods

3.1. Geomorphological mapping

The geomorphological map of the Blidinje Polje (~100 km^2) was performed in detail by Stepišnik et al. (2016), who used a 20 m–resolution digital elevation model (DEM), Google Earth images and topographic maps at a scale of 1: 25,000 and orthophotos (Geoportal Web Preglednik, 2016). Limited geomorphological and geological descriptions of the area (Milićević and Prskalo, 2014; Milojević, 1935; Roglić, 1959), and maps of landmine contamination from the 1992–1995 war, obtained from Bosnia and Herzegovina Mine Action Centre, were also essential while performing the fieldwork. We based our study on the results of Stepišnik et al. (2016) and sampled 2 areas where the moraines were most promising for cosmogenic ^{36}Cl surface exposure dating because of their degree of preservation.

3.2. Cosmogenic nuclide dating

In the karstic Blidinje Polje moraines, we applied ^{36}Cl cosmogenic surface exposure dating method to estimate the retreat timing of the glaciers. The length of time that the boulder has been exposed on the moraine surfaces can be estimated using certain cosmogenic nuclides (such as ^{36}Cl, ^{10}Be and ^{26}Al) (Davis and Schaeffer, 1955; Dunai, 2010). Here, we used ^{36}Cl because the carbonates suit well to the production of ^{36}Cl.

Dating carbonates with ^{36}Cl depends on the interactions of secondary fast neutrons, thermal and epithermal neutrons and negative slow muons with the nuclides in rocks (mainly, ^{40}Ca, ^{39}K and ^{35}Cl). Measured ^{36}Cl concentrations in rocks can be used to quantify the time–length of boulder exposition (Gosse and Phillips, 2001; Owen et al., 2001).

3.2.1. Sample collection and preparation

We collected 12 samples for cosmogenic ^{36}Cl dating from the top of the boulders on the crests of lateral, terminal and hummocky moraines. Large embedded boulders on moraine crests were preferred to sustain stability and preservation of boulders. We concentrated on the largest moraines that were reasonably away from the minefields; hence safe enough to accomplish the fieldwork. A few cm thick rock samples were chipped out from boulder tops by hammer and chisel (Table 1). Shielding of surrounding topography was measured by inclinometer from the horizon at each sample location (Gosse and Phillips, 2001).

Table 1: Sample locations, attributes and local corrections to production rates.

	Sample ID	Latitude (WGS84)	Longitude (WGS84)	Elevation*	Boulder dimensions (LxWxH)	Sample thickness	Topography correction factor
		°N (DD)	°E (DD)	(m)	(m)	(cm)	
1	SV16-01	43,5929	17,4654	1252	3x1.5x1	3	0,9964
2	SV16-02	43,5943	17,4693	1257	1.5x1x0.8	2	0,9958
3	SV16-03	43,5957	17,4727	1240	3x2x1.2	2	0,9982
4	SV16-04	43,5922	17,4653	1252	1x2x1	3	0,9964
5	SV16-05	43,5898	17,4658	1242	1.3x1x0.8	2	0,9843
6	SV16-06	43,5874	17,4745	1302	1x1x0.5	4	0,9771
7	SV16-07	43,5875	17,4741	1307	1.5x1x0.6	3	0,9771
8	SV16-08	43,5877	17,4733	1298	0.6x1x0.4	3	0,9771
9	GL16-01	43,6321	17,5315	1285	1x1x0.4	2	0,9896
10	GL16-02	43,6363	17,5299	1271	1.5x1.5x0.8	4	0,9963
11	GL16-03	43,6480	17,5374	1278	0.5x0.4x0.25	4	0,9982
12	GL16-04	43,6366	17,5302	1268	2.5x2x1	3	0,9927

*Elevation data is based on hand-held GPS measurements. Thus, uncertainty on elevation was taken as ±5 m.

The samples were prepared at Istanbul Technical University's (ITU) Kozmo–Lab (http://www.kozmo–lab.itu.edu.tr/en) facility according to procedures described in Sarıkaya (2009). The crushed samples at appropriate grain size (0.25–1 mm) were leached with deionized water and 10% HNO_3 to remove secondary carbonates, dust and organic particles. Aliquots of leached samples were used to measure the major and minor element concentrations at the Acme Lab (ActLabs Inc., Ontario Canada) (Table 2). Spiked (~99% ^{35}Cl enriched $Na^{35}Cl$ from Aldrich Co., USA) samples were digested with excess amount of 2 M HNO_3 in 500 ml HDPE bottles (Sarıkaya et al., 2014; Schlagenhauf et al., 2010). ~10 ml of 0.1 M $AgNO_3$ solution was added before the digestion to precipitate AgCl. Sulphur was removed from the solution by repeated precipitation of $BaSO_4$ with addition of $Ba(NO_3)$ and re–acidifying with concentrated HNO_3. Final precipitates of AgCl were sent to the ANSTO, Accelerated Mass Spectrometer (AMS) in Sydney, Australia for isotope ratio measurements given in Supplementary Table S1. Total Cl was determined by isotope dilution method (Desilets et al., 2006; Ivy–Ochs et al., 2004) after AMS analysis (Table 2).

Table 2: Geochemical analytical data.

	Sample ID	Major elements											Trace elements					
		Al_2O_3	CaO	Fe_2O_3	K_2O	MgO	MnO	Na_2O	P_2O_5	SiO_2	TiO_2	CO_2 (LOI)	Sm	Gd	U	Th	Cl	
		(wt. %)	(wt. %)	(wt. %)	(wt. %)	(wt. %)	(wt. %)	(wt. %)	(wt. %)	(wt. %)	(wt. %)	(wt. %)	(ppm)	(ppm)	(ppm)	(ppm)	(ppm)	
1	SV16-01	0,18	54,45	0,15	0,03	0,56	0,01	0,03	0,04	0,56	0,01	43,90	0,11	0,16	2,40	0,20	13,6 ±	1,3
2	SV16-02	0,07	55,12	0,08	0,01	0,48	0,02	0,01	0,04	0,39	0,01	43,70	0,13	0,16	0,80	0,20	14,0 ±	1,3
3	SV16-03	0,05	54,80	0,09	0,01	0,72	0,02	0,01	0,10	0,50	0,01	43,60	0,13	0,11	0,60	0,20	11,7 ±	1,1
4	SV16-04	0,05	55,34	0,07	0,01	0,44	0,01	0,01	0,05	0,36	0,01	43,60	0,11	0,18	0,80	0,20	9,1 ±	0,8
5	SV16-05	0,12	54,92	0,07	0,01	0,52	0,01	0,02	0,01	0,48	0,01	43,70	0,05	0,05	2,10	0,20	13,2 ±	1,2
6	SV16-06	0,06	54,98	0,06	0,01	0,67	0,01	0,01	0,01	0,26	0,01	43,90	0,05	0,06	1,60	0,20	18,5 ±	1,7
7	SV16-07	0,03	55,29	0,06	0,01	0,58	0,01	0,02	0,01	0,15	0,01	43,80	0,05	0,05	1,80	0,20	16,4 ±	1,5
8	SV16-08	0,01	55,32	0,06	0,01	0,51	0,01	0,01	0,01	0,21	0,01	43,80	0,05	0,05	2,10	0,20	5,6 ±	0,5
9	GL16-01	0,02	54,85	0,06	0,01	0,88	0,01	0,03	0,01	0,18	0,01	43,90	0,05	0,05	8,30	0,20	39,0 ±	3,5
10	GL16-02	0,03	55,28	0,07	0,01	0,53	0,01	0,02	0,01	0,24	0,01	43,80	0,05	0,05	2,80	0,20	56,6 ±	5,1
11	GL16-03	0,02	55,30	0,06	0,01	0,58	0,01	0,01	0,01	0,16	0,01	43,80	0,07	0,09	0,50	0,20	25,3 ±	2,3
12	GL16-04	0,04	54,81	0,04	0,01	0,71	0,01	0,02	0,01	0,40	0,01	43,90	0,05	0,05	5,10	0,20	28,7 ±	2,6

3.2.2 Determination of ^{36}Cl ages

The CRONUS Web Calculator version 2.0 (http://www.cronuscalculators.nmt.edu) (Marrero et al., 2016a) was used to calculate sample ages. Cosmogenic ^{36}Cl production rates of Marrero et al. (2016b) [56.3 ± 4.6 atoms ^{36}Cl (g Ca)$^{-1}$ a^{-1} for Ca spallation, 153 ± 12 atoms ^{36}Cl (g K)$^{-1}$ a^{-1} for K spallation and 743 ± 179 fast neutrons (g air)$^{-1}$ a^{-1}] were scaled using the time–dependent Lifton–Sato–Dunai schema (also called "LSD" or "SF" scaling) (Lifton et al., 2014). We used 190 µ g^{-1} a^{-1} for slow negative muon stopping rate at land surface at sea–level high–latitude (Heisinger et al., 2002). ~95% of ^{36}Cl production is due to the spallation and negative muon capture reactions on ^{40}Ca. Because of the low Cl concentration of our samples (<57 ppm), thermal neutron capture reactions by ^{35}Cl constitute only ~5% of the total ^{36}Cl production. Lower Ca spallation production rates suggested by Stone et al. (1996) or Schimmelpfennig et al. (2011) will make our ages ~10% older. All essential information to reproduce resultant ages is given in Supplementary Table S1.

All surface exposure ages include corrections for thickness and topographic shielding. We reported both zero–erosion and 40 mm ka^{-1} erosion corrected boulder ages and preferred to use the latter, as the study area is located in one of the highest precipitation regions of Europe

(>2000 mm yr^{-1}), and boulder surfaces show up to several cm deep solution grooves. Snow thicknesses were estimated based on meteorological data from the Nevesinje weather station (Data courtesy Federal Hydrometeorological Institute, Sarajevo) (Table 3). Thus, snow correction factor for spallation reactions of 0.9539 was applied to all samples based on snowpack of 25, 100, 100, 100, 50, 25 cm of snow on Nov, Dec, Jan, Feb, Mar and Apr on top of boulders (Table 3) using the snow density of 0.25 g cm^{-3}, and spallation attenuation length of 170 g cm^{-2}. Please note that these estimates are minimum snowpack values since the precipitation at sampling elevations might be higher that the precipitation measurements at Nevesinje station. Doubling the snowpack make the correction factor 0.9131, and make the ages ~9% older.

Table 3: Meteorological data obtained from measurements at Nevesinje station (~40 km southeast of the study area) used to estimate the snow depth on top of the sampled boulders.

Months	I	II	III	IV	V	VI	VII	VIII	IX	X	XI	XII
Temperature, °C, at Nevesinje station (@900 m asl)	-0,9	0,5	3,5	7,5	12,3	15,5	18,0	17,8	14,2	9,7	4,8	0,5
Precipitation, mm, at Nevesinje station	171	169	165	162	119	97	65	85	116	178	242	225
Snow depth, cm, measured at Nevesinje station	117	70	53	34	4	0	0	0	0	10	30	65
Temperature @1270 m asl using 6.5 °C km^{-1} temp. lapse rate	-3,3	-1,9	1,1	5,1	9,9	13	16	15	12	7,3	2,4	-1,9
Minimum snow water equivalent, mm (=prec, if temp<0)	171	169	0	0	0	0	0	0	0	0	0	225
Minimum snow depth, cm (using the 10:1 snow depth ratio)	171	169	0	0	0	0	0	0	0	0	0	225
Our snowpack estimates on top of boulders (aver. boulder height 70 cm)	**100**	**100**	**50**	**25**	**0**	**0**	**0**	**0**	**0**	**0**	**25**	**100**

4. Results

4.1. Glacial geomorphology

The Blidinje Polje is filled with different types of sediments derived from the steep slopes of Vran Mountain (2074 m a.s.l.) to the northwest and Čvrsnica Mountain (2226 m a.s.l.) to the southeast (Figure 1). In detail the Blidinje Polje can be further classified as a border–type polje because of inflows from fluviokarst areas as well as a piedmont–type polje due to former inflows from glaciated areas (Ford and Williams, 2007; Gams, 1978). The Blidinje Lake (1180 m a.s.l.) in the south has abrasion terraces up to 7 m above the mean lake level indicating its larger extent in the past. The reader is referred to Stepišnik et al. (2016) for a

detailed geomorphological map and description of the Blidinje Polje and surrounding areas. Postglacial subsurface drainage into karst is well developed in the areas of palaeoglaciers, therefore products of past glaciations are well preserved (Smart, 2004; Žebre and Stepišnik, 2015). Glacial deposits in form of lateral, terminal and hummocky moraines, mostly in north and northwest facing slopes of Vran and Čvrsnica mountains, are present in the study area (Stepišnik et al., 2016). Few km^2 large proglacial fans, with glacial outwash sediments, are also found just below these moraines. Out of six major moraine depositional areas, we have chosen only two sample areas, where moraines were most promising for a chronological reconstruction. The presence of different types of moraines, boulder availability and accessibility, and clear evidence of multiple glacial advances also influenced our choice.

4.1.1. Svinjača area

The area southwest of Blidinje Polje is known as Svinjača and is surrounded by the foothills of Vran Mountain to the north and western Čabulja Mountain to the south (Stepišnik et al., 2016) (Figure 2). Svinjača area is ~3.5 km long and up to 1.5 km wide, with a flat floor at an elevation of ~1170 m. A palaeoglacier, ~6 km long, that originated from a small ice cap (estimated to ~8x5 km) above 1400 m a.s.l., occupied the glacial valley at the southwestern part of the Čvrsnica Mountain, and is responsible for the deposition of the hummocky moraines found at Svinjača area (Figure 3a). The hummocky moraine morphology left behind by gradually melting piedmont glacier is characterized by more or less equally–distributed, randomly–oriented chaotic mounds and depressions, which do not show any specific organization (e.g. knob and kettle topography described by Gravenor and Kupsch, 1959). Up to 10 m high and 10–50 m wide mounds, with ~20^o upper surface slopes, are separated by 10–50 m wide and several meters deep irregular depressions. Hummocky moraines are composed of Cretaceous limestone pebbles and cobbles (10 to 50 cm in diameter), but larger blocks of 1 to 3 m in diameter are also observed. The latter were preferred for sampling, although having

signs of surface weathering. The depressions are filled by finer material and a thin veneer of black soil is present with grassy vegetation.

A left lateral moraine ~400 m long and ~30 m high (to 1265 m a.s.l.) is also found at the termination of the glacial valley (Figure 3b–d). The lateral moraine extends from 1300 m a.s.l. down to 1265 m a.s.l., and is composed of diamicton characterized by unsorted and unstratified sandy–silty matrix with subangular to subrounded boulders of limestone.

At the northwestern limit of the palaeo–piedmont lobe, which is represented by the hummocky morphology, a proglacial fan, with flatter topography and finer grained sediments, covers a large section of the Svinjača floor. As no surface streams are found in the Svinjača depression, Stepišnik et al. (2016) interpreted the area as a combination of piedmont and border–type polje owing to the presence of fluviokarst and proglacial deposits filling the polje (Ford and Williams, 2007; Gams, 1978).

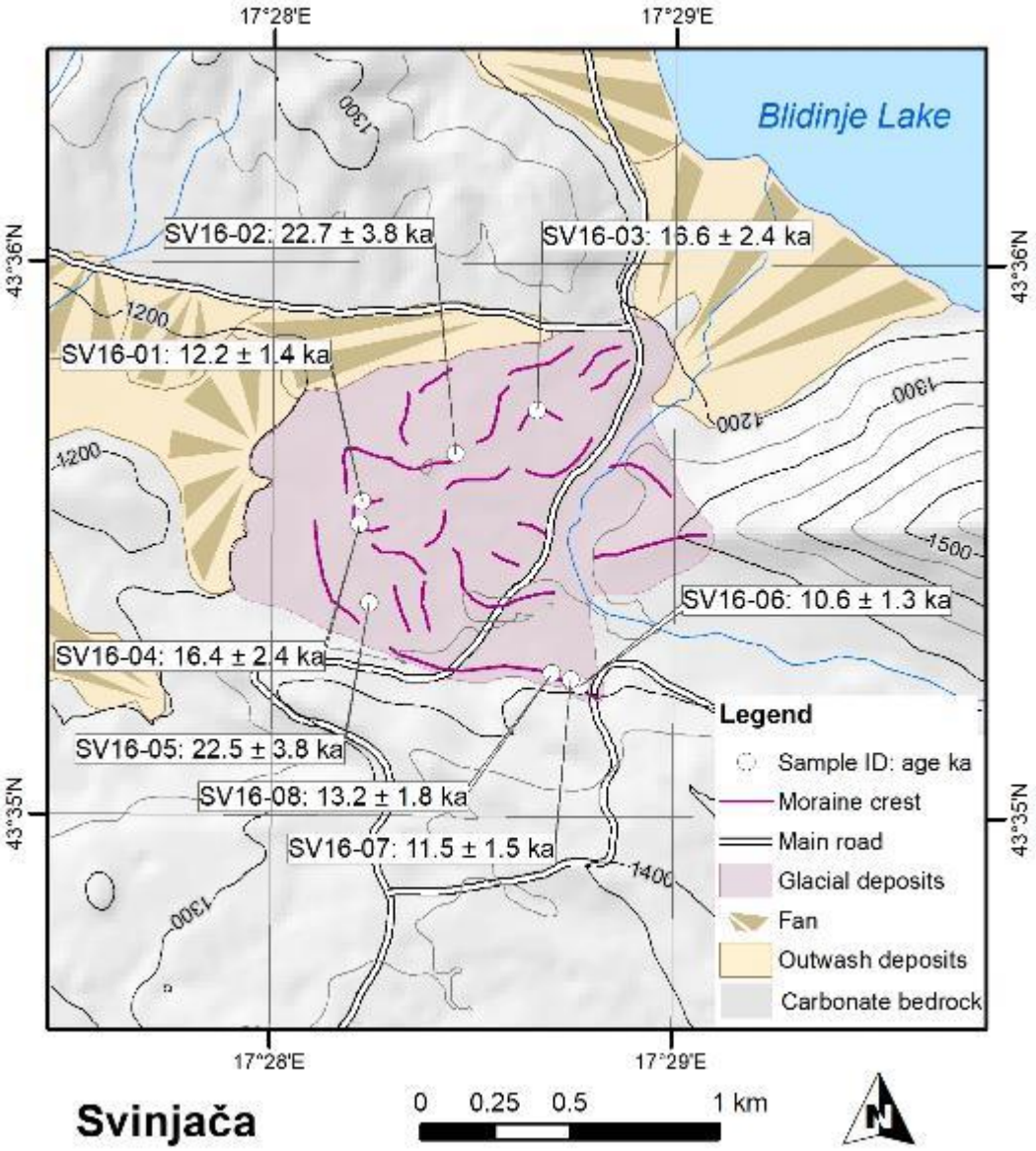

Figure 2: Geomorphological map of glacial landforms in the Svinjača area. Samples for ^{36}Cl cosmogenic nuclide dating were collected from the hummocky (SV16–01 to SL16–05) and left lateral (SV16–06 to SL16–08) moraines. The samples ID`s along with the ages (ka) corrected for 40 mm ka^{-1} of erosion are also shown on the map.

Figure 3: Svinjača area moraines; a) Typical view of the hummocky moraines (HM) with knob and kettle topography. Blidinje Lake is seen at the horizon (photo looking to northeast), b) left lateral (LLM) and hummocky moraines (HM) (photo looking to W), c) exit of the glacial and the left lateral moraine (LLM) (photo looking to E), d) cross section of the lateral moraine with unsorted and unstratified limestone boulders floating in a sandy matrix. White and red arrows indicate palaeo–ice flow directions. Houses (a, b, c) and person (d) for scale.

4.1.2. Glavice area

A typical amphitheater shaped terminal moraine, here named as Glavice moraine, oriented in a southeast to northwest direction and ~3 km in diameter, constitutes one of the largest moraine complexes of the Blidinje Polje (Figures 4 and 5a–c). This moraine complex that descends down to 1260 m a.s.l. at its lowermost northeastern extent, was probably deposited by a small outlet glacier originating from the Čvrsnica ice cap. Although the moraine is well preserved, dense dwarf mountain pine vegetation with a thick black soil cover makes a detailed observation and sampling rather difficult. Cretaceous and Jurassic limestone and dolostone boulders (1 to 3 m in diameter) can be observed between the trees and were sampled when adequate. Today, two major but inactive streambeds, formed by proglacial streams flowing towards northwest, dissect the outer rim of the moraine loop. To the northwest and north of the moraine, outwash fans cover parts of Blidinje Polje.

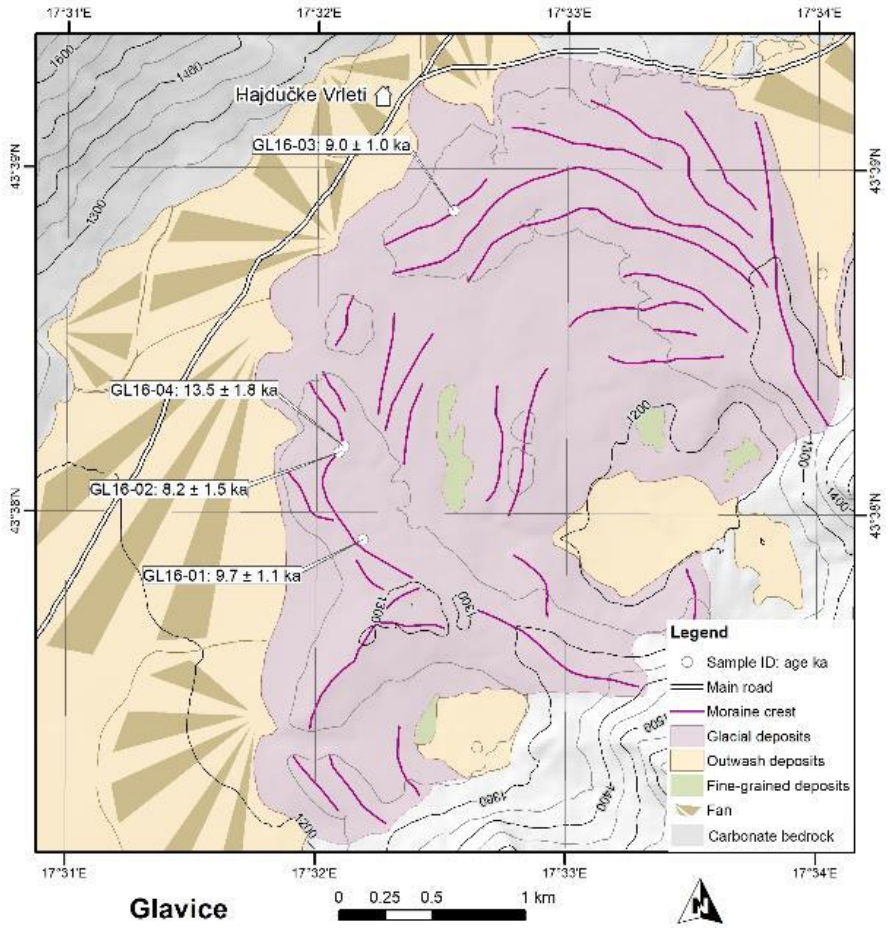

Figure 4: Geomorphological map of glacial landforms in the Glavice area. Samples for ^{36}Cl cosmogenic nuclide dating were collected from the terminal moraine complex (GL16–01 to GL16–04). The samples ID`s along with the ages (ka) corrected for 40 mm ka^{-1} of erosion are also shown on the map.

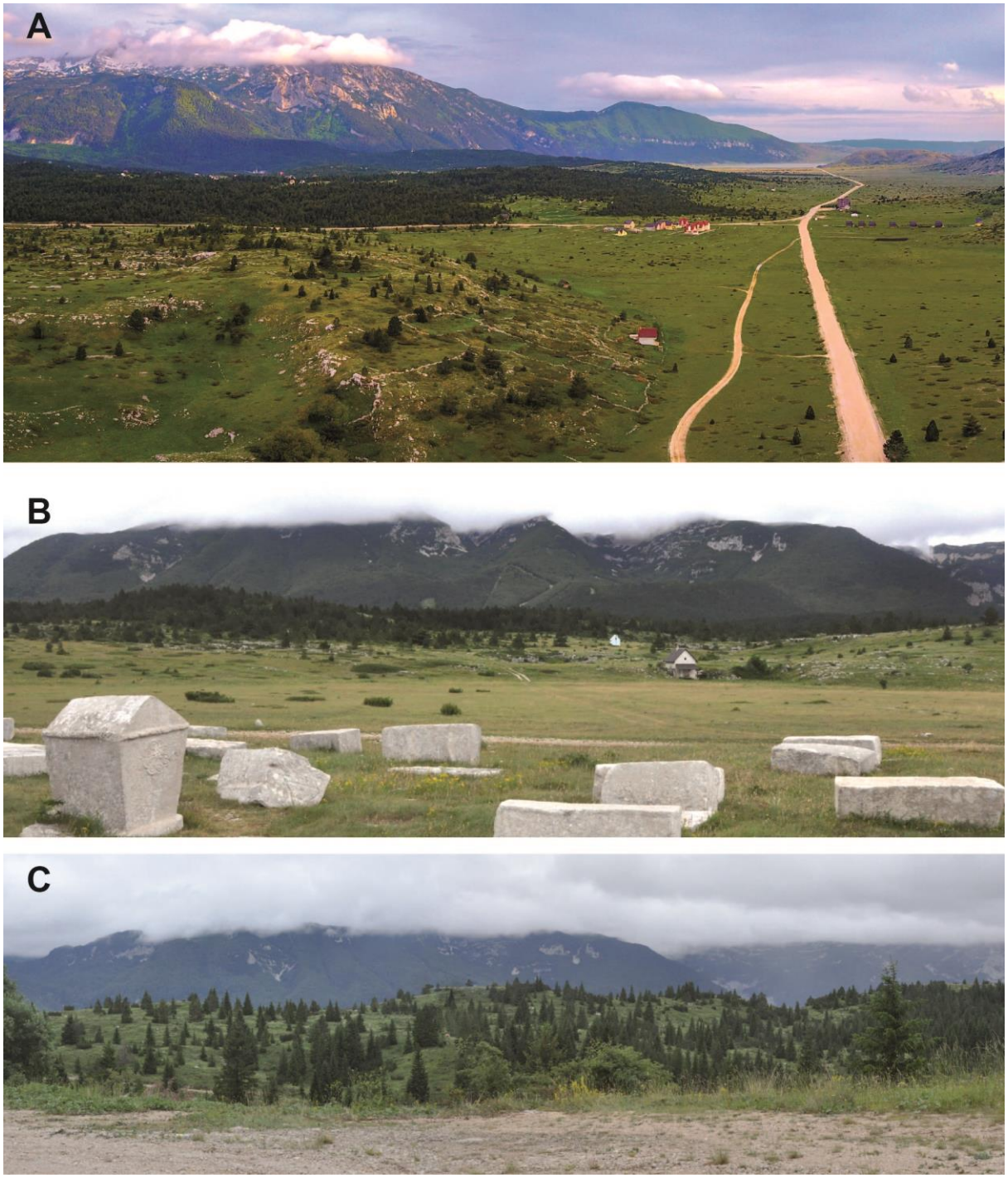

Figure 5: Glavice terminal moraine pictures; a) a typical amphitheater shaped terminal moraine (overgrown by forest) covering part of the Blidinje Polje (view from northeast towards southwest), b) the frontal view of terminal moraine with Stećak –monumental Medieval (12^{th} – 15^{th} Century) tombstones found scattered across BIH, inscribed as UNESCO's World Heritage Site since 2016– at the foreground, c) close–up view of the terminal moraines.

4.2. ^{36}Cl exposure ages and Blidinje area chronology interpretation

We collected a total of 12 glacial boulder samples from Svinjača and Glavice areas for ^{36}Cl cosmogenic nuclide dating purposes (Table 1). We used 40 mm ka^{-1} as the most representative erosion rate for the correction of all sample ages as denudation rates of carbonate rocks can be very high and are enhanced with increasing mean annual precipitation (MAP) (Levenson et al., 2017; Ryb et al., 2014). This seemingly high denudation rates are to be expected in areas where very high mean annual precipitations are observed (Levenson et al., 2017), such as Nevesinje nearby the study area. Comparable denudation rates (30–60 mm ka^{-1}) were also measured in the Mediterranean karst in southeastern France (Thomas et al., 2018) independently of the precipitation amount. We preferred to use the same erosion rate as in Velež and Crvanj mountains (Žebre et al., 2019), only ~40 km away. However, we recognize that such high erosion rates (40 mm ka^{-1}) will inevitably limit the confidence in the corrected ages, especially for older periods. We present age uncertainties at the 1–sigma level (i.e. one standard deviation), which include both the analytical and production rate errors (i.e. total uncertainties). We used the oldest moraine boulder age as the age of that landform, which represent the beginning of glacier retreat (Figure 8).

4.2.1. Svinjača glacial chronology

Five samples from the hummocky moraines and 3 samples from the left lateral moraine were collected at the exit of the glacial valley (Figure 6). The chemical analysis of all samples collected from this area is almost identical; limestone, showing similar concentrations of CaO (~55%) and very low K_2O (0.01%) and Cl (5.6–12.8 ppm), thus the main production mechanism (>97%) is spallation of Ca (Table 2, Supplementary Table S1). Five boulders from the hummocky moraines yielded ^{36}Cl ages of 12.2 ± 1.4 ka (SV16–01), 22.7 ± 3.8 ka (SV16–02), 16.6 ± 2.4 ka (SV16–03), 16.4 ± 2.4 ka (SV16–04) and 22.5 ± 3.8 ka (SV16–05) (Table 4). The oldest moraine boulder age is 22.7 ± 3.8 ka and indicates the Last Glacial Maximum (LGM; the time period when ice masses reached their last maximum global extent at around 23–19 ka (Hughes et al., 2013)) as the retreat time of the piedmont glacier (Figure 8). On the other hand, boulders from the left lateral moraine gave ^{36}Cl ages of 10.6 ± 1.3 ka (SV16–06), 11.5 ± 1.5 ka (SV16–07) and 13.2 ± 1.8 ka (SV16–08) (Table 4). Here, the oldest moraine boulder age is 13.2 ± 1.8 ka, and indicates the moraine formation during the Younger Dryas stadial within error. As expected, the left lateral moraine is younger than the hummocky moraines as it is found on higher elevation at the exit of the glacial valley.

Figure 6: Photos of the sampled boulders and their ages from the Svinjača hummocky (SV16–01 to SV16–05) and lateral moraines (SV16–06 to SV16–08).

4.2.2. Glavice glacial chronology

We also collected 4 samples from the terminal moraine of the Glavice area (Figure 7). Boulders have similar carbonate lithologies (55% CaO) with slightly higher Cl concentrations (~37 ppm) than samples from Svinjača. Four boulders of the terminal moraine complex yielded ^{36}Cl ages of 9.7 ± 1.1 ka (GL16–01), 8.2 ± 1.5 ka (GL16–02), 9.0 ± 1.0 ka (GL16–03) and 13.5 ± 1.8 ka (GL16–04) (Table 4). Here we applied the same approach as in Svinjača and chose the oldest boulder age (13.5 ± 1.8 ka) from the terminal moraine as the most representative time of moraine emplacement. This age indicates the Younger Dryas stadial within error in the Glavice area.

Figure 7: Photos of the sampled boulders and their ages from the Glavice terminal moraine complex (GL16–01 to GL16–04).

Table 4: Cosmogenic ^{36}Cl inventories and ages of boulders considering 0 mm ka^{-1} and 40 mm ka^{-1} erosion rates. Landform ages of moraines are based on the oldest sample's 40 mm ka^{-1} erosion corrected age in the Svinjača and Glavice areas.

	Sample ID	Landform	^{36}Cl (measured)	Surface Exposure Ages		Landform Age
				Erosion corrected (0 mm ka^{-1})	Erosion corrected (40 mm ka^{-1})	
			(10^4 atoms g^{-1} rock)	(ka)	(ka)	(ka)
Svinjača						
1	SV16-01	Hummocky Moraine	49,28 ± 1,63	8,7 ± 0,8	12,2 ± 1,4	
2	SV16-02	Hummocky Moraine	72,19 ± 2,44	12,7 ± 1,1	**22,7 ± 3,8**	
3	SV16-03	Hummocky Moraine	59,22 ± 2,21	10,6 ± 1,0	16,6 ± 2,4	**22.7 ± 3.8**
4	SV16-04	Hummocky Moraine	58,31 ± 2,28	10,4 ± 0,9	16,4 ± 2,4	
5	SV16-05	Hummocky Moraine	69,78 ± 2,23	13,0 ± 1,0	22,5 ± 3,8	
6	SV16-06	Lateral Moraine	46,90 ± 1,78	8,0 ± 0,7	10,6 ± 1,3	
7	SV16-07	Lateral Moraine	49,82 ± 1,73	8,4 ± 0,7	11,5 ± 1,5	**13.2 ± 1.8**
8	SV16-08	Lateral Moraine	50,76 ± 2,18	8,9 ± 0,8	**13,2 ± 1,8**	
Glavice						
9	GL16-01	Terminal Moraine	50,98 ± 1,86	8,0 ± 0,6	9,7 ± 1,1	
10	GL16-02	Terminal Moraine	47,46 ± 5,91	7,0 ± 1,0	8,2 ± 1,5	**13.5 ± 1.8**
11	GL16-03	Terminal Moraine	43,47 ± 1,65	7,3 ± 0,6	9,0 ± 1,0	
12	GL16-04	Terminal Moraine	58,80 ± 1,91	9,9 ± 0,9	**13,5 ± 1,8**	

The proposed boulder and moraine ages should be considered as minimum ages as suggested also by other studies (e.g. Ivy–Ochs and Schaller, 2009; Lukas, 2011; Lüthgens et al., 2011) (Figure 8). We also think that the dated left lateral and terminal moraines in both areas belong to the same glacial period within error (Younger Dryas) not only because they have very close cosmogenic ages (13.2 ± 1.8 ka and 13.5 ± 1.8 ka, respectively), but also because they are found at similar elevations (~1300 m a.s.l.).

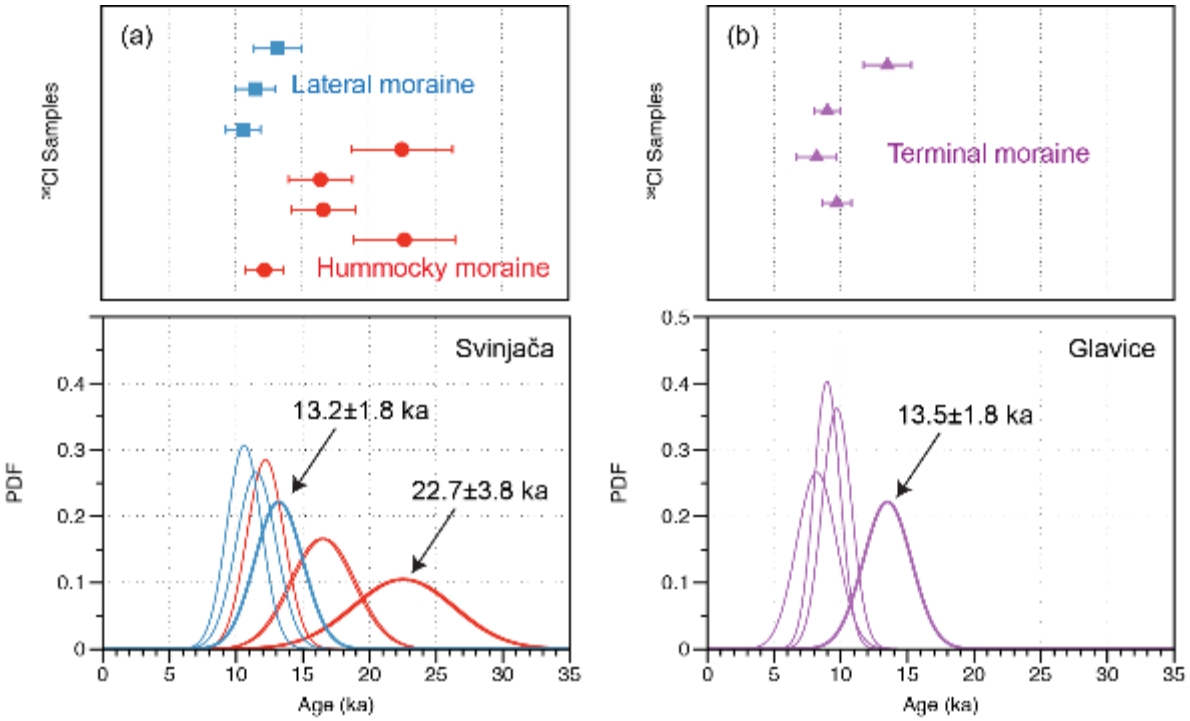

Figure 8: Cosmogenic ^{36}Cl ages of the boulders from (a) hummocky moraines and left–lateral (LLM) moraines of Svinjača and (b) terminal moraines of Glavice areas. Upper panels show the individual sample ages with 1–sigma uncertainties, and the lower panels show the probably density functions (PDF) of the samples. Oldest age of the moraines (indicated by thick PDF curves) from both data sets were shown and assigned to the age of the landforms.

5. Discussion

5.1. Interpreting the moraine age from the boulders

Numerous studies suggest different approaches (i.e. taking the oldest boulder age within a cluster or weighted average age of boulders after the exclusion of outliers etc…) for the interpretation of a moraine landform age from the dated boulders (e.g. D'Arcy et al., 2019; Applegate et al., 2010, 2012; Çiner et al., 2017; Davis et al., 1999; Dortch et al., 2013; Hallet and Putkonen, 1994; Heyman et al., 2011; May et al., 2011; Putkonen and Swanson, 2003; Žebre et al., 2019; Zech et al., 2017). In our study we prefer to use the oldest boulder age as

the most representative age of the landform, because the exhumation and erosion of boulders are the main geological uncertainties to be considered while interpreting exposure ages in very humid environments, such as our study area. However, further discussion of these methods is out of the scope of this paper and we refer the readers to Žebre et al. (2019) for a detailed discussion related to this problematic, especially focused on the climatic conditions specific to the Dinaric Mountains. Other discussions on the interpretation of boulder ages within a moraine can be found in Palacios et al. (2019), and in the Appendix of D'Arcy et al. (2019).

5.2. Piedmont glaciers and hummocky moraines

The term "hummocky moraine" is very useful for describing the overall appearance of many areas of moraines in formerly glaciated areas (Hughes, 2004). The supraglacial debris cover is at the origin of the hummocky moraines, which is a descriptive term that designates moundy, irregular morainic knob–and–kettle (convex and concave) topography (e.g. Gravenor and Kupsch, 1959; Aario, 1977; Sharp, 1985; Çiner et al., 1999; Benn and Owen, 2002). Hummocky moraines have been described in several locations in the world; e.g. in Scotland (Sissons (1967), in Turkey (Çiner, 2003; Çiner et al., 1999, 2015), in Tajikistan (Zech et al., 2005) and in Norway (Knudsen et al., 2006).

Different interpretations exist about the formation of hummocky moraines; they can result from locally isolated patches of melting glaciers (Clapperton and Sugden, 1977), melting of debris–covered ice in ice–cored moraines (Lukas, 2011), or subglacial deformation of coarse debris including older till deposits (Hodgson, 1982). For instance Sissons (1967, 1979) described hummocky moraines in Scotland as "chaotic mounds that lack any systematic arrangement" and interpreted this as evidence of *in situ* glacier stagnation. This view was later challenged by several other studies, which argued that the hummocky moraine topography could be also formed by the decay of detached ice–blocks from an actively retreating glacier

(Eyles, 1983; Bennett and Glasser, 1991; Bennett and Boulton, 1993; Bennett, 1990, 1994). Hummocky moraines can be also the result of combined processes, such as in Lenin Peak (Pamir Mountains, Kyrgyzstan), where two different geomorphic events have been inferred from hummocky terrain (landslide, glacier) even if they look very similar (Oliva and Ruiz–Fernández, 2018). Some authors even argue that hummocky moraines could also form subglacially by the overburden pressure of stagnant ice (e.g. Boone and Eyles, 2001).

Hummocky accumulations in the Svinjača area are likely the result of the melting debris–covered glacier snout. Ice ablation caused transport of debris away from topographic heights on the glacier surface by mass movement resulting in an irregular mounds and ridges topography. Sedimentology of hummocky moraines is normally complex due to multiple cycles of re–deposition during their formation and parallel reworking with meltwater streams (Benn and Evans, 2010). Lack of glaciofluvial and lacustrine deposits interbedded with supraglacial till in the outcrops in the case of Svinjača area is probably the result of reduced meltwaters action due to active vertical drainage into karst. Additionally, part of knob–and–kettle topography in the area is due to suffusion process, where till is evacuated trough underlying pipes into karst (Ford and Williams, 2007). Boulders from the hummocky moraines in the Svinjača area indicate the LGM as the formation time of the piedmont glacier. On the other hand, boulders from the left lateral moraine in the Svinjača area and terminal moraine in the Glavice area are younger and indicate a deglaciation during the Younger Dryas. Although a two–phase interpretation might hold true, we should also take into account different moraine degradation rates and their effect on the exhumation processes. Sharp–crested and steep lateral moraines are normally affected by higher degree of post–glacial degradation and boulder exhumation than small, flat crested hummocky moraines (Applegate et al., 2010; Putkonen and Swanson, 2003). As a result, the cosmogenic age does not always reflect a true moraine age, but instead the age of the boulder exhumation, especially in the

case of steep lateral moraines.

It should also be noted that even though the oldest ages obtained from the lateral and terminal moraines in both areas overlap within error with the Younger Dryas stadial, they could also fall within the preceding Allerød, which was a warm and moist interstadial that occurred between ~13.9 ka to ~12.9 ka ago. For instance in Scotland's last ice fields a similar age dataset was reinterpreted as indicating a larger Allerød glacier extent and retreat during the Younger Dryas stadial (Bromley et al. 2014, 2018). However, as the Younger Dryas stadial is recorded throughout the Mediterranean mountains glacial records (e.g. Çiner and Sarıkaya, 2017; Hughes et al., 2018), it seems likely that this was also the case in our study area.

5.3 Glacial chronologies in the Balkans

Glaciation extent of the western Balkan Mountains has been adequately studied, but there is relatively little morphochronologic data to associate with the Blidinje area. Some of the glacial records in the Balkans have been dated using U–series (Adamson et al., 2014; Hughes et al., 2006, 2007, 2010, 2011) that gives a minimum age for the glacial deposits by dating secondary carbonates, which are formed after the formation of the host moraines (Figure 9 and Table 5). Unlike U–series, cosmogenic dating has the potential to obtain the depositional age of a moraine and thus can provide a more precise geochronology for the Late Pleistocene glaciations. This method has been applied to some areas in the western and southern Balkans (Kuhlemann, 2009, 2013; Pope et al., 2015; Styllas et al., 2018). However, there is a considerable scatter in dataset between and amongst U–series and cosmogenic dating (Table 5).

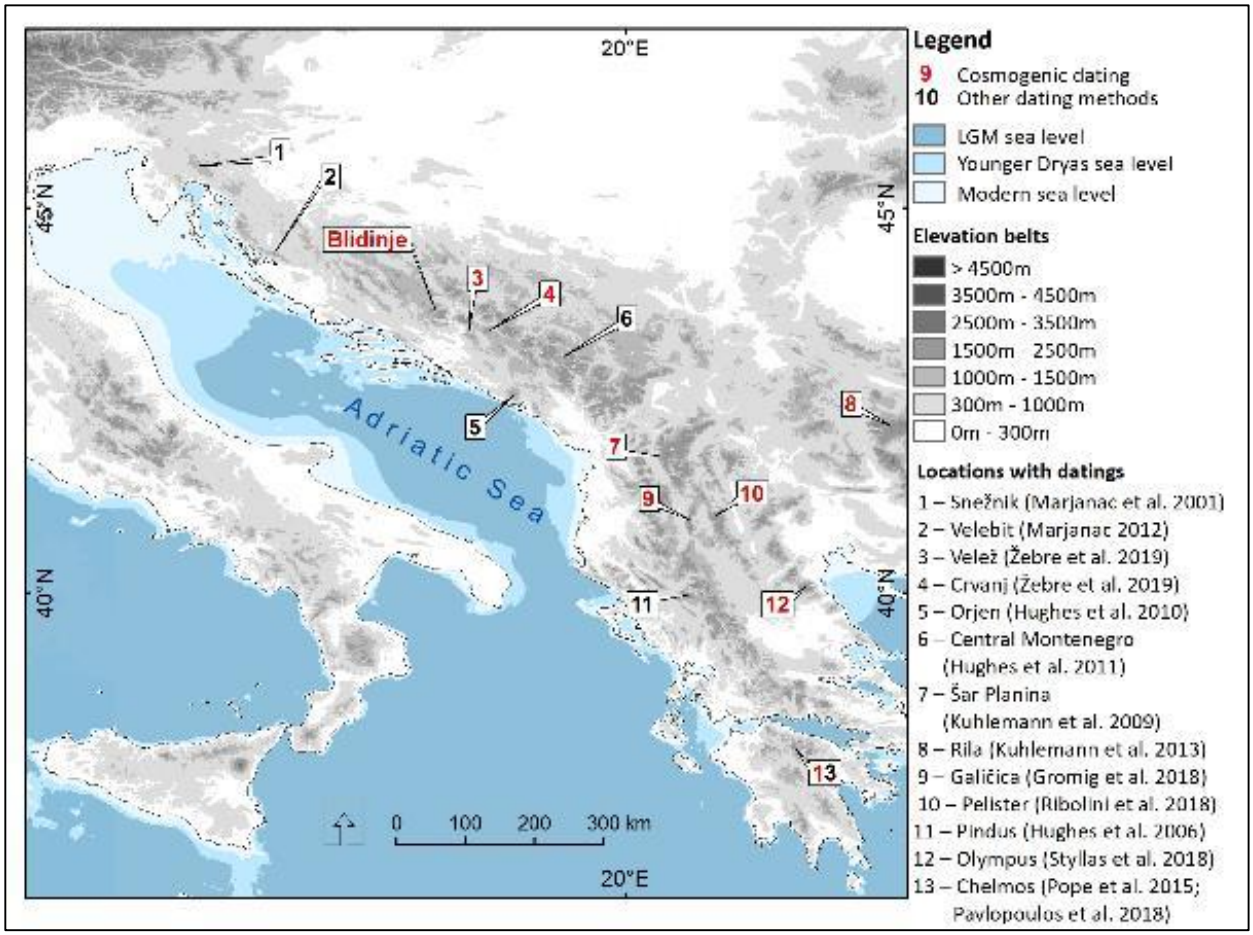

Figure 9: (a) All locations in the Balkan Peninsula where moraines and outwash deposits have been dated so far. Base layer of mountain belts is from https://ilias.unibe.ch/goto.php?target=file_1049915, based on the mountain definition by Kapos et al. (2000). Bathymetric data is from the European Marine Observation and Data Network (http://www.emodnet.eu/), while the sea level data for LGM and Younger Dryas is from Lambeck et al. (2011).

Table 5: A list of different dating methods applied to glacial landforms in the Balkan Peninsula (modified from Žebre et al., 2019).

Mountain	Dating method	Age	Erosion rate	Number of samples	Reference
Snežnik (Croatia)	^{14}C	LGM (18.7 ±1.0 cal kyr BP*)	/	1 (animal bone in outwash fan)	Marjanac et al., 2001
Pindus (Greece)	U–series	MIS 12 (>350–71 ka), MIS 6 (131.3–80.5 ka)	/	28 from at least 11 landforms (calcite cement from moraines and alluvial deposits)	Hughes et al., 2006; Woodward et al., 2004
Šar Planina (FYROM)	^{10}Be cosmogenic exposure dating	LGM (19.4 ± 3.2 ka to 12.4 ± 1.7 ka), Younger Dryas (14.7 ± 2.1 to 11.9 ± 1.7 ka)	10 mm/ka	8 from at least 6 landforms (moraine boulders)	Kuhlemann et al., 2009
Orjen (Montenegro)	U–series	MIS 12 (>350–324.0 ka), MIS 6 (124.6–102.4 ka), MIS 5d–2 (17.3–12.5 ka), Younger Dryas (9.6–8.0 ka)	/	12 from 7 landforms (calcite cement from moraines)	Hughes et al., 2010
Central Montenegro	U–series	MIS 12 (>350 ka; 396.6–38.8 ka), MIS 8 or 10 (231.9–58.8 ka), MIS 6 (120.2–88.1 ka) MIS 2 (13.4 ka), Younger Dryas (10.9–2.2 ka)	/	19 from 11 landforms (calcite cement from moraines)	Hughes et al., 2011
Velebit mountain, Velebit channel (Croatia)	U–series	MIS 12–6 (>350–61.5 ka)	/	9 from at least 6 landforms (calcite cement from moraines, paleocaverns, former ice wedges)	Marjanac, 2012
Rila (Bulgaria)	^{10}Be cosmogenic exposure dating	LGM (23.5–14.4 ka)	0 mm/ka	10 from at least 6 landforms (moraine boulders)	Kuhlemann et al., 2013
Chelmos (Greece)	**^{36}Cl cosmogenic exposure dating**	MIS 3 (39.9 ± 3.0 ka to 30.4 ± 2.2 ka), LGM (22.9 ±1.6 ka to 21.2 ± 1.6 ka), Younger Dryas (12.6 ± 0.9 ka to 10.2 ± 0.7 ka)	0 mm/ka	7 from 4 different landforms (moraine boulders)	Pope et al., 2015
Galičica (FYROM)	**^{36}Cl cosmogenic exposure dating**	Younger Dryas (12.8 ± 1.4 ka to 11.3 ± 1.3)	5 mm/ka	5 from 1 landform (moraine boulders)	Gromig et al., 2018
Pelister (FYROM)	^{10}Be cosmogenic exposure dating	Oldest Dryas (15.56 ± 0.85 to 15.03 ± 0.85)	0 mm/ka	3 from 1 landform (moraine boulders)	Ribolini et al., 2018

Olympus (Greece)	**^{36}Cl cosmogenic exposure dating**	Lateglacial (3 phases: 15.5 ± 2.0 ka, 13.5 ± 2.0 ka, 12.5 ± 1.5 ka), Holocene (3 phases: 9.6 ± 1.1 ka, 2.5 ± 0.3 ka, 0.64 ± 0.08ka)	0 mm/ka	20 from 11 landforms (moraine boulders, bedrock)	Styllas et al., 2018
Velež and Crvanj (Bosnia and Herzegovina)	**^{36}Cl cosmogenic exposure dating**	Oldest Dryas (14.9 ± 1.1 ka) Younger Dryas j (11.9 ± 0.9 ka)	40 mm/ka	20 from7 landforms (moraine boulders)	Žebre et al., 2019

Recent studies using ^{36}Cl cosmogenic dating from the adjacent massifs yielded ages spanning from Oldest Dryas (14.9 ± 1.1 ka) for the Velež Mountain to Younger Dryas (11.9 ± 0.9 ka) for the Crvanj Mountain with maximum extent of glacial deposits located as low as ~900 m a.s.l. (Žebre et al., 2019).

Another area where the ^{36}Cl cosmogenic nuclide dating technique was used is Mount Chelmos in Greece, which yielded the last phase of moraine building within local cirques at the Younger Dryas to Early Holocene (13–10 ka). Lower glacial deposits at ~2100 m a.s.l. indicate that the glacial maximum of the last cold stage occurred during MIS 3 (40–30 ka), several thousand years before the global LGM at MIS 2 (Pope et al., 2015). On the contrary, ground moraines at the same elevation in a parallel valley yielded optically stimulated luminescence (OSL) ages of MIS–5b (89–86 ka) (Pavlopoulos et al., 2018). The lowest glacial deposits reaching elevations of ~1200 m a.s.l. were not dated, but they are assumed to be of Middle Pleistocene age (Pope et al., 2015). On Mount Olympus in Greece at an elevation of ~2200 m a.s.l., glacier retreat phases were dated within cirque moraines by ^{36}Cl cosmogenic method that can be correlated to the Oldest Dryas (~15.5 ka) and Younger Dryas (~12.5 ka). Although, there are no chronological data for the maximum glacial extent the LGM moraines were assumed to be a short distance away at the entrance to the cirque (Sytllas et al., 2018). The older Middle Pleistocene glaciations were found in much lower altitudes extending well beyond the high mountain area down to the piedmont (Smith et al., 1997).

Glacial chronologies, based on the cosmogenic nuclide dating were established also for the Galičica, Šar Planina, and Pelister mountains in North Macedonia. In the Galičica Mountain, ^{36}Cl ages of moraine boulders at an elevation of ~2050 m a.s.l. indicate a moraine formation in the course of the Younger Dryas (12.0 ± 0.6 ka), while moraines further down valley at an elevation of 1550 m a.s.l. were not dated (Gromig et al., 2018). Results of ^{10}Be cosmogenic exposure dating applied to the cirque moraine in the Pelister Mountain (North Macedonia) at an elevation of 2215 m a.s.l. demonstrate the Oldest Dryas age (15.24 ± 0.85 ka), whereas stratigraphically older moraines were not dated (Ribolini et al., 2018). The age of moraine boulders in the Šar Planina Mountain was determined by ^{10}Be cosmogenic exposure dating (Kuhlemann et al., 2009). The maximum glacier advances that reached elevations between 1100 and 1500 m a.s.l. were correlated to the LGM (22.5–20 ka). Moraines at altitudes between 1600 and 2200 m were linked with the Oldest Dryas (16.5–15 ka), while moraines at altitudes between 2100 and 2400 m with the Younger Dryas (~12 ka). Small local moraines at higher elevation, close to the crest, were tentatively attributed to the 8.2 ka event (Kuhlemann et al., 2009). ^{10}Be cosmogenic exposure dating was used to date the moraine boulders also in the Rila Mountain in Bulgaria. The maximum glaciation extent at an elevation between 1150 and 2000 m a.s.l. yielded ages prior (~25–23 ka) and after (~18–16 ka) LGM (Kuhlemann et al., 2013).

U–series dating technique was applied to date glacial deposits in Montenegro and Greece, where the two largest most palaeoglacier extents were correlated with MIS 12 (480–430 ka) and MIS 6 (190–130 ka) Middle Pleistocene cold stages (Hughes et al., 2006, 2007, 2010, 2011). Glaciers of the last cold stage have been recorded only in the form of limited–extent cirque glaciers, which is consistent with the findings using the same dating technique from the northern Greece (Hughes et al., 2007).

Our glacial chronological data from the Blidinje area are in good agreement with other cosmogenic nuclide dating data from other parts of the Balkan Peninsula. ^{36}Cl ages from hummocky moraines in the Svinjača area indicate first ever–reported LGM age of the glaciers in Bosnia and Herzegovina, which roughly corresponds to the established cosmogenic ^{10}Be chronologies from the Rila and Šar Planina mountains (Kuhlemann et al., 2009, 2013). Younger Dryas ages from the lateral and terminal moraines in Blidinje are in good agreement with the dating results from the Velež Mountain (Žebre et al., 2019), Mount Olympus (Styllas et al., 2018), and Galičica Mountains (Gromig et al., 2018).

In the future special priority should be given to quartz–rich lithologies in the dating of moraine boulders in prevalently carbonate mountains in the Balkans, such was done by Ribolini et al. (2018) in Mount Pelister in North Macedonia. This would then test and verify ^{36}Cl–based ages, and help confirm the validity of 40 mm ka^{-1} erosion rate that we used in our study. On that regard, it is interesting to note that Mount Pelister's quartz rich schist moraines (no boulder erosion assumed) yield an Oldest Dryas age, whereas limestone moraines in very closely situated Galičica Mountains at similar altitude, where 5 mm ka^{-1} boulder erosion rate was assumed, are Younger Dryas in age (Gromig et al., 2018). Whether this difference is due to variations in lithologies and/or erosion rates, or indicates a real difference in glacial chronology is an open question that needs to be answered by future research. Therefore, it is clear that more quantitative age results are needed from neighbouring countries in order to better understand the glacial history of the Dinaric Mountains.

6. Conclusions

The Blidinje Polje in the Dinaric Mountains of Bosnia and Herzegovina along the eastern Adriatic coast was glaciated during the Late Pleistocene. A piedmont glacier that originated from the Čvrsnica Mountain (2226 m a.s.l.) descended down to 1250 m in the Svinjača area,

and covered a surface of ~1.5 km^2. Hummocky and lateral moraines composed of limestone boulders up to 3 m in diameter, were later deposited by the melting of this glacier lobe. Because of dissolution susceptible limestone lithology and very high precipitation in the area, we used 40 mm ka^{-1} bedrock erosion rate, and dated the moraine boulders by cosmogenic ^{36}Cl surface exposure method. The results indicate the first ever reported LGM (22.7 ± 3.8 ka) extent of glaciers from the Dinaric Mountains in Bosnia and Herzegovina. The lateral moraine of this piedmont lobe apparently developed during the Younger Dryas (13.2 ± 1.8 ka) stadial within error. Within the Blidinje Polje in Glavice area, another amphitheater shaped terminal moraine, at similar altitudes, yielded a similar Younger Dryas (13.5 ± 1.8 ka) age within error, confirming the importance of this stadial in this part of Dinaric Mountains.

7. Acknowledgements

This work was supported by the Istanbul Technical University Research Fund (project MGA–2017–40540), by the Scientific and Technological Research Council of Turkey (TÜBİTAK–118Y052) and by the Slovenian Research Agency (research core funding No. P1–0011, P6–0229(A) and P1–0025), by the Department of Geography, University of Ljubljana. Nevesinje climate data are provided courtesy of the Federal Hydrometeorological Institute, Sarajevo, Bosnia and Herzegovina. We are very thankful to Klaus Wilcken at the ANSTO Lab in Australia for AMS measurements. We also acknowledge laboratory assistance of Oğuzhan Köse (Istanbul Technical University). We thank reviewers Marc Oliva and Philip Hughes, and editor Catherine Kuzucuoğlu for their helpful suggestions that improved the quality of the paper.

References

Aario, R. 1977. Classification and terminology of morainic landforms in Finland. Boreas 6, 87–100.

Adamson, K.R., Woodward J.C., Hughes P.D. 2014. Glaciers and rivers: Pleistocene uncoupling in a Mediterranean mountain karst. Quaternary Science Reviews 94, 28–43.

Applegate, P.J., Urban, N.M., Keller, K., Lowell, T.V., Laabs, B.J.C., Kelly, M.A., Alley, R.B. 2012. Improved moraine age interpretations through explicit matching of geomorphic process models to cosmogenic nuclide measurements from single landforms. Quatarnary Research 77, 293–304. https://doi.org/10.1016/J.YQRES.2011.12.002

Applegate, P.J., Urban, N.M., Laabs, B.J.C., Keller, K., Alley, R.B. 2010. Model Development Modeling the statistical distributions of cosmogenic exposure dates from moraines. Geoscientific Model Development 3, 293–307.

Benn, D.I. Owen, L.A. 2002. Himalayan glacial sedimentary environments: a framework for reconstructing and dating the former extent of glaciers in high mountains, Quaternary International 97–98, 3–25.

Benn, D.I., Evans, D.J.A. 2010. Glaciers and Glaciation. Rutledge, New York, 802–802.

Bennett, M.R. 1990. The deglaciation of Glen Croulin, Knoydart. Scottish Journal of Geology 26, 41–46.

Bennett, M.R. 1994. Morphological evidence as a guide to deglaciation following the Loch Lomond Stadial: a review of research approaches and models. Scottish Geographical Magazine 110, 24–32.

Bennett, M.R., Boulton, G.S. 1993. A reinterpretation of Scottish "hummocky moraine" and its significance for the deglaciation of the Scottish Highlands during the Younger Dryas

or Loch Lomond Stadial. Geological Magazine 130, 301–318.

Bennett, M.R., Glasser, N.F. 1991. The glacial landforms of Glen Geusachan, Cairngorms: a reinterpretation. Scottish Geographical Magazine 107, 116–123.

Boone, S.J., Eyes, N. 2001. Geotechnical model for great plains hummocky moraine formed by till deformation below stagnant ice. Geomorphology 38, 109–124.

Bromley, G. R. M., Putnam, A. E., Rademaker, K. M., Lowell, T. V., Schaefer, J. M., Hall, B. L., et al. 2014. Younger Dryas deglaciation of Scotland driven by warming summers. Proceedings of the National Academy of Sciences of the United States of America 111, 17, 6215–6219. https://doi.org/10.1073/pnas.1321122111

Bromley, G., Putnam, A., Borns, H.Jr, Lowell, T., Sandford, T., Barrell, D. 2018. Interstadial rise and Younger Dryas demise of Scotland's last ice fields. Paleoceanography and Paleoclimatology 33, 412–429. https://doi.org/10.1002/2018PA003341

Buljan, R., Zelenika, M., Mesec, J. 2005. Park prirode Blidinje, prikaz geološke građe i stukturno–tektonskih odnosa [Geologic and tectonic settings of the park of nature Blidinje]. In I. Čolak (Ed.), Prvi međunarodni znanstveni simpozij Blidinje 2005 (11–24). Mostar: Građevinski fakultet Sveučilišta u Mostaru.

Çiner, A. 2003. Sedimentary facies analysis and depositional environments of the Late Quaternary moraines in Geyikdağ (Central Taurus Mountains). Geological Bulletin of Turkey 46, 1, 35–54 (in Turkish).

Çiner, A., Deynoux, M., Çörekçioğlu, E. 1999. Hummocky moraines in the Namaras and Susam valleys, Central Taurids, SW Turkey. Quaternary Science Reviews 18, 4–5, 659–669.

Çiner, A., Sarıkaya, M.A., Yıldırım, C. 2015. Late Pleistocene piedmont glaciations in the Eastern Mediterranean; insights from cosmogenic ^{36}Cl dating of hummocky moraines in

southern Turkey. Quaternary Science Reviews 116. 44–56. https://doi.org/10.1016/j.quascirev.2015.03.017

Çiner, A., Sarıkaya, M.A., Yıldırım, C. 2017. Misleading old age on a young landform? The dilemma of cosmogenic inheritance in surface exposure dating: Moraines vs. rock glaciers. Quaternary Geochronology 42, 76–88. https://doi.org/10.1016/J.QUAGEO.2017.07.003

Clapperton, C.M., Sugden, D.E. 1977. The late Devensian glaciation of North East Scotland. In: Gray, J.M., Lowe, J.J. (Eds.), Studies in the Scottish Lateglacial Environment. Pergamon, Oxford, 1–4.

Cvijić, J. 1899. Glacijalne i morfološke studije o planinama Bosne, Hercegovine i Crne Gore (Glacial and Morphological Studies about Montains of Bosnia, Herzegovina and Montenegro). Srpska kraljevska akademija, Beograd, 57 pp.

Cvijić, J. 1900. Karsna polja zapadne Bosne i Hercegovine (Die Karstpoljen in Westbosnien und in Herzegowina). Glas Srpske kraljevske akademije nauka, 59, 1, 59–182.

D'Arcy, M. Schildgen, T.F., Strecker, M.R., Wittmann, H., Duesing, W., Mey, J., Tofelde, S., Weissmann, P., Alonso, R.N. 2019. Timing of past glaciation at the Sierra de Aconquija, northwestern Argentina, and throughout the Central Andes. Quaternary Science Reviews 204, 37–57.

Davis, P.T., Bierman, P.R., Marsella, K.A., Caffee, M.W., Southon, J.R. 1999. Cosmogenic analysis of glacial terrains in the eastern Canadian Arctic: a test for inherited nuclides and the effectiveness of glacial erosion. Annals of Glaciology 28, 181–188. https://doi.org/10.3189/172756499781821805

Davis, R., Schaeffer, O.A. 1955. Chlorine–36 in nature. Ann. N. Y. Acad. Sci. 62, 107–121.

Desilets, D., Zreda, M., Almasi, P.F., Elmore, D. 2006. Determination of cosmogenic ^{36}Cl in

rocks by isotope dilution: innovations, validation and error propagation. Chemical Geology 233, 185–195. https://doi.org/10.1016/J.CHEMGEO.2006.03.001

Dortch, J.M., Owen, L.A., Caffee, M.W. 2013. Timing and climatic drivers for glaciation across semi–arid western Himalayan–Tibetan orogen. Quaternary Science Reviews 78, 188–208. https://doi.org/10.1016/J.QUASCIREV.2013.07.025

Dunai, T. 2010. Cosmogenic Nuclides Principles, Concepts and Applications in the Earth Surface Sciences. Cambridge Academic Press.

Eyles, N. 1983. Modern Icelandic glaciers as depositional models for hummocky moraines in the Scottish Highlands. In: Evenson, E.B., Schlüchter, C., Rabassa, J. (Eds.), Tills and Related Deposits. Balkema, 47–60.

Ford, D., Williams, P.D. 2007. Karst Hydrogeology and Geomorphology. Wiley, Chichester, 576 p.

Gams, I. 1978. The polje: the problem of definition: with special regard to the Dinaric karst. Zeitschrift für Geomorphologie, 22, 2, 170–181.

Geoportal Web Preglednik 2016. In: F.u.z.g.i.i.–p. poslove (Editor). Federalna uprava za geodetske i imovinsko–pravne poslove, Sarajevo.

Gosse, J.C., Phillips, F.M. 2001. Terrestrial in situ cosmogenic nuclides: theory and application. Quaternary Science Reviews 20, 1475–1560. https://doi.org/10.1016/S0277–3791(00)00171–2

Gravenor, C.P., Kupsch, W.O. 1959. Ice–disintegration features in Western Canada. Journal of Geology 67, 48–64.

Gromig, R., Mechernich, S., Ribolini, A., Wagner, B., Zanchetta, G., Isola, I., Bini, M., Dunai, T.J. 2018. Evidence for a Younger Dryas deglaciation in the Galičica Mountains (FYROM) from cosmogenic ^{36}Cl. Quaternay International 464, 352–363.

https://doi.org/10.1016/j.quaint.2017.07.013

Grund, A. 1902. Neue Eiszeitspuren aus Bosnien und der Hercegovina. Globus 81, 149–150.

Grund, A. 1910. Beiträge zur Morphologie des Dinarischen Gebirges, in: Geographische Abhandlungen. B. G. Teubner, Berlin, p. 230.

Gunn, J. 2004. Erosion rates: field measurements, in: Gunn, J. (Ed.), Encyclopedia of Caves and Karst Science. Fitzroy Dearborn, New York, London, 664–668.

Hallet, B., Putkonen, J. 1994. Surface Dating of Dynamic Landforms: Young boulders on aging moraines. Science 265, 5174, 937–940. https://doi.org/10.1126/science.265.5174.937

Heisinger, B., Lal, D., Jull, A.J.T., Kubik, P., Ivy–Ochs, S., Knie, K., Nolte, E. 2002. Production of selected cosmogenic radionuclides by muons: 2. Capture of negative muons. Earth Planetary Science Letters 200, 357–369. https://doi.org/10.1016/S0012–821X(02)00641–6

Heyman, J., Stroeven, A.P., Harbor, J.M., Caffee, M.W. 2011. Too young or too old: Evaluating cosmogenic exposure dating based on an analysis of compiled boulder exposure ages. Earth Planetary Science Letters 302, 71–80. https://doi.org/10.1016/J.EPSL.2010.11.040

Hodgson, D.M. 1982. Hummocky and fluted moraines in parts of northwest Scotland. Ph.D. thesis, University of Edinburgh.

Hughes, P., Gibbard, P.L., Ehlers, J. 2013. Timing of glaciation during the last glacial cycle: evaluating the concept of a global “Last Glacial Maximum” (LGM). Earth–Science Reviews 125, 171–198.

Hughes, P.D. 2004. Quaternary Glaciation in the Pindus Mountains, Northwest Greece. Ph.D. thesis, University of Cambridge, 341 p.

Hughes, P.D., Fink, D., Rodés, Á., Fenton, C.R., Fujioka, T. 2018. ^{10}Be and ^{36}Cl exposure ages and palaeoclimatic significance of glaciations in the High Atlas, Morocco. Quaternary Science Reviews 180, 193–213.

Hughes, P.D., Gibbard, P.L., Woodward, J.C. 2007. Geological controls on Pleistocene glaciation and cirque form in Greece. Geomorphology 88, 3, 242–253.

Hughes, P.D., Woodward, J.C. 2017. Quaternary glaciation in the Mediterranean mountains: a new synthesis. Geological Society London, Spec. Publ. 433, 1–23. https://doi.org/10.1144/SP433.14

Hughes, P.D., Woodward, J.C., Gibbard, P.L., Macklin, M.G., Gilmour, M.A., Smith, G.R. 2006. The Glacial History of the Pindus Mountains, Greece. Journal of Geology 114, 413–434. https://doi.org/10.1086/504177

Hughes, P.D., Woodward, J.C., van Calsteren, P.C., Thomas, L.E. 2011. The glacial history of the Dinaric Alps, Montenegro. Quaternary Science Reviews 30, 3393–3412. https://doi.org/10.1016/j.quascirev.2011.08.016

Hughes, P.D., Woodward, J.C., van Calsteren, P.C., Thomas, L.E., Adamson, K.R. 2010. Pleistocene ice caps on the coastal mountains of the Adriatic Sea. Quaternary Science Reviews 29, 3690–3708. https://doi.org/10.1016/j.quascirev.2010.06.032

Ivy–Ochs, S., Schaller, M. 2009. Examining Processes and Rates of Landscape Change with Cosmogenic Radionuclides. Radioact. Environ. Chapter 6, 16, 231–294. https://doi.org/10.1016/S1569–4860(09)01606–4

Ivy–Ochs, S., Synal, H.–A., Roth, C., Schaller, M. 2004. Initial results from isotope dilution for Cl and ^{36}Cl measurements at the PSI/ETH Zurich AMS facility. Nucl. Instruments Methods Phys. Res. Sect. B Beam Interact. with Mater. Atoms 223–224, 623–627. https://doi.org/10.1016/J.NIMB.2004.04.115

Kapos, V., Rhind, J., Edwards, M., Price, M., Ravilious, C. 2000. Developing a map of the world's mountain forests, in: Price, M., Butt, N. (Eds.), Forests in Sustainable Mountain Development: A Report for 2000. CAB International, Wallingford, 4–9. https://doi.org/10.1007/1–4020–3508–X_52

Knudsen, C.G., Larsen, E., Sejrup, H.P., Stalsberg, K. 2006. Hummocky moraine landscape on Jæren, SW Norway–implications for glacier dynamics during the last deglaciation. Geomorphology 77, 153–168.

Kottek, M., Grieser, J., Beck, C., Rudolf, B., Rubel, F. 2006. World Map of the Köppen–Geiger climate classification updated. Meteorol. Zeitschrift 15, 259–263. https://doi.org/10.1127/0941–2948/2006/0130

Krklec, K., Domínguez–Villar, D., Perica, D. 2015. Depositional environments and diagenesis of a carbonate till from a Quaternary paleoglacier sequence in the Southern Velebit Mountain (Croatia). Palaeogeography Palaeoclimatology Palaeoecology 436, 188–198. https://doi.org/10.1016/J.PALAEO.2015.07.004

Kuhlemann, J., Gachev, E., Gikov, A., Nedkov, S., Krumrei, I., Kubik, P. 2013. Glaciation in the Rila mountains (Bulgaria) during the Last Glacial Maximum. Quaternary International 293, 51–62. https://doi.org/10.1016/J.QUAINT.2012.06.027

Kuhlemann, J., Milivojević, M., Krumrei, I., Kubik, P.W. 2009. Last glaciation of the Šara Range (Balkan peninsula): Increasing dryness from the LGM to the Holocene. Austrian J. Earth Science 102, 1, 146–158.

Lambeck, K., Antonioli, F., Anzidei, M., Ferranti, L., Leoni, G., Scicchitano, G., Silenzi, S. 2011. Sea level change along the Italian coast during the Holocene and projections for the future. Quaternaty International 232, 250–257. https://doi.org/https://doi.org/10.1016/j.quaint.2010.04.026

Levenson, Y., Ryb, U., Emmanuel, S. 2017. Comparison of field and laboratory weathering rates in carbonate rocks from an Eastern Mediterranean drainage basin. Earth Planetary Science Letters 465, 176–183. https://doi.org/10.1016/j.epsl.2017.02.031

Liedtke, V.H. 1962. Vergletscherungsspuren und Periglazialerscheinungen am Südhang des Lovcen östlich von Kotor. Eiszeitalter und Gegenwart 13, 15–18.

Lifton, N., Sato, T., Dunai, T.Journal 2014. Scaling in situ cosmogenic nuclide production rates using analytical approximations to atmospheric cosmic–ray fluxes. Earth Planetary Science Letters 386, 149–160. https://doi.org/10.1016/J.EPSL.2013.10.052

Lukas, S. 2011. Ice–cored moraines. In: Singh, V., Singh, P., Haritashya, U.K. (Eds.), Encyclopedia of Snow, Ice and Glaciers. Springer, Heidelberg, 616–619.

Lüthgens, C., Böse, M., Preusser, F. 2011. Age of the Pomerian ice–marginal position in northeastern Germany determined by Optically Stimulated Luminescence (OSL) dating of glaciofluvial sediments. Boreas 40, 598–615.

Marjanac, L., Marjanac, T. 2004. Glacial history of the Croatian Adriatic and coastal Dinarides. In: Ehlers, J., Gibbard, P.L. (Eds.), Quaternary Glaciations – Extent and Chronology. Part I: Europe. Elsevier, Amsterdam, 19–26.

Marković, M. 1973. Geomorfološka evolucija i neotektonika Orjena. Rudarsko Geološki Fakultet, Beograd, 269 pp.

Marrero, S.M., Phillips, F.M., Borchers, B., Lifton, N., Aumer, R., Balco, G. 2016a. Cosmogenic nuclide systematics and the CRONUScalc program. Quaternary Geochronology 31, 160–187. https://doi.org/10.1016/j.quageo.2015.09.005

Marrero, S.M., Phillips, F.M., Caffee, M.W., Gosse, J.C. 2016b. CRONUS–Earth cosmogenic ^{36}Cl calibration. Quaternary Geochronology 31, 199–219. https://doi.org/10.1016/j.quageo.2015.10.002

Milićević, M., Prskalo, M. 2014. Geomorfološki tragovi pleistocenske glacijacije na Čvrsnici [Geomorphological Traces of Pleistocene Glaciation of the Čvrsnica Massif], e–Zbornik – Elektronički zbornik radova Građevinskog fakulteta, 87–94.

Milojević, B.Ž. 1935. Čvrsnica. Hrvatski geografski glasnik 6, 1, 17–23.

Oliva, M., Ruiz–Fernández, J. 2018. Late Quaternary environmental dynamics in Lenin Peak area (Pamir Mountains, Kyrgyzstan). Science of the Total Environment 645, 603–614.

Owen, L.A., Gualtieri, L., Finkel, R.C., Caffee, M.W., Benn, D.I., Sharma, M.C. 2001. Cosmogenic radionuclide dating of glacial landforms in the Lahul Himalaya, northern India: defining the timing of Late Quaternary glaciation. Journal of Quaternary Science 16, 555–563. https://doi.org/10.1002/jqs.621

Palacios, D., Gómez–Ortiz, A. Alcalá–Reygosa, J., Andrés, N., Oliva, M., Tanarro, L.M., Salvador–Franch, F., Schimmelpfennig, I., Léanni, L., ASTER Team 2019. The challenging application of cosmogenic dating methods in residual glacial landforms: the case of Sierra Nevada (Spain). Geomorphology 325, 103–118.

Pavlopoulos, K., Leontaritis, A., Athanassas, C.D., Petrakou, C., Vandarakis, D., Nikolakopoulos, K., Stamatopoulos, L., Theodorakopoulou, K. 2018. Last glacial geomorphologic records in Mt Chelmos, North Peloponnesus, Greece. Journal of Mountain Science 15, 5, 948–965.

Penck, A. 1900. Die Eiszeitspuren auf der Balkanhalbinsel. Globus 78, 133–178.

Petrović, A.S. 2014. A Reconstruction of the Pleistocene Glacial Maximum in the Žijovo Range (Prokletije Mountains, Montenegro). Acta Geographica Slovenica 54, 256–269. https://doi.org/https://doi.org/10.3986/AGS54202

Pope, R.J., Hughes, P.D., Skourtsos, E. 2015. Glacial history of Mt Chelmos, Peloponnesus, Greece. Geological Society of London Special Publication 433, 211–236.

https://doi.org/10.1144/SP433.11

Putkonen, J., Swanson, T. 2003. Accuracy of cosmogenic ages for moraines. Quaternay Research 59, 255–261. https://doi.org/10.1016/S0033–5894(03)00006–1

Reimer, P.J., Bard, E., Bayliss, A., Beck, J.W., Blackwell, P.G., Bronk Ramsey, C., Buck, C.E., Cheng, H., Edwards, R.L., Friedrich, M., Grootes, P.M., Guilderson, T.P., Haflidason, H., Hajdas, I., Hatt_e, C., Heaton, T.J., Hoffmann, D.L., Hogg, A.G., Hughen, K.A., Kaiser, K.F., Kromer, B., Manning, S.W., Niu, M., Reimer, R.W., Richards, D.A., Scott, E.M., Southon, J.R., Staff, R.A., Turney, C.S.M., van der Plicht, J. 2013. IntCal13 and Marine13 Radiocarbon Age Calibration Curves 0–50,000 Years cal BP. Radiocarbon 55, 1869–1887. https://doi.org/10.2458/azu_js_rc.55.16947.

Ribolini, A., Bini, M., Isola, I., Spagnolo, M., Zanchetta, G., Pellitero, R., Mechernich, S., Gromig, R., Dunai, T., Wagner, B., Milevski, I. 2018. An Oldest Dryas glacier expansion on Mount Pelister (Former Yugoslavian Republic of Macedonia) according to ^{10}Be cosmogenic dating. Journal Geological Society London. https://doi.org/10.1144/jgs2017–038

Riđanović, J. 1966. Orjen – La montagne dinarique. Radovi geografskog instituta sveučilišta u Zagrebu. Geografski institut, Prirodoslovno–matematički fakultet, Zagreb.

Roglić, J. 1959. Prilog poznavanju glacijacije i evolucije reljefa planina oko srednje Neretve (Supplement to the Knowledge of Glaciation and Relief Evolution of the Mountains Near Middle Neretva River). Geografski glasnik 21, 1, 9–34.

Ryb, U., Matmon, A., Erel, Y., Haviv, I., Benedetti, L., Hidy, A.J. 2014. Styles and rates of long–term denudation in carbonate terrains under a Mediterranean to hyper–arid climatic gradient. Earth Planetary Science Letters 406, 142–152.

https://doi.org/10.1016/J.EPSL.2014.09.008

Sarıkaya, M.A. 2009. Late Quaternary glaciation and paleoclimate of Turkey inferred from cosmogenic ^{36}Cl dating of moraines and glacier modeling. PhD thesis. University of Arizona, USA.

Sarıkaya, M.A., Çiner, A. 2017. The late Quaternary glaciation in the Eastern Mediterranean. In: "Quaternary Glaciation in the Mediterranean Mountains". Hughes, P. & Woodward, J. (eds.), Geological Society of London Special Publication 433, 289–305, http://doi.org/10.1144/SP433.4

Sarıkaya, M.A., Çiner, A., Haybat, H., Zreda, M. 2014. An early advance of glaciers on Mount Akdağ, SW Turkey, before the global Last Glacial Maximum; insights from cosmogenic nuclides and glacier modeling. Quaternary Science Reviews 88, 96–109. https://doi.org/10.1016/J.QUASCIREV.2014.01.016

Sawicki, L. von. 1911. Die eiszeitliche Vergletscherung des Orjen in Süddalmatien. Zeitscrift für Gletscherkunde 5, 339–355.

Schimmelpfennig, I., Benedetti, L., Garreta, V., Pik, R., Blard, P.–H., Burnard, P., Bourlès, D., Finkel, R., Ammon, K., Dunai, T. 2011. Calibration of cosmogenic ^{36}Cl production rates from Ca and K spallation in lava flows from Mt. Etna (38°N, Italy) and Payun Matru (36°S, Argentina). Geochimica et Cosmochimica Acta 75, 2611–2632. https://doi.org/10.1016/j.gca.2011.02.013

Schlagenhauf, A., Gaudemer, Y., Benedetti, L., Manighetti, I., Palumbo, L., Schimmelpfennig, I., Finkel, R., Pou, K. 2010. Using in situ Chlorine–36 cosmonuclide to recover past earthquake histories on limestone normal fault scarps: a reappraisal of methodology and interpretations. Geophysical Journal International 182, 36–72. https://doi.org/10.1111/j.1365–246X.2010.04622.x

Sharp, M.J. 1985. Sedimentation and stratigraphy at Eyjabakkajøkull: an icelandic surging glacier. Quaternary Research 24, 268–284.

Sissons, J.B. 1967. The Evolution of Scotland's Scenery. Oliver and Boyd, Edinburgh. Younger Dryas or Loch Lomond Stadial. Geological Magazine 130, 301–318.

Sissons, J.B. 1979. The Loch Lomond Stadial in the British Isles. Nature 280, 199–203.

Smart, C.C. 2004. Glacierized and glaciated karst. In: J. Gunn (Editor), Encyclopedia of caves and karst science. Fitzroy Dearborn, New York, 804–809.

Smith, G.W., Nance, R.D. Genes, A.N. 1997. Quaternary glacial history of Mount Olympus. Geological Society of America Bulletin 109, 809–824.

Sofilj, J., Živanović, M. 1979. Osnovna geološka karta SFRJ. K 33–12, Prozor [Basic Geological Map of SFRJ. K 33–12, Prozor]. Savezni geološki zavod, Beograd.

Stepišnik, U., Ferk, M., Kodelja, B., Medenjak, G., Mihevc, A., Natek, K., Žebre, M. 2009. Glaciokarst of western Orjen. Cave and Karst Science 36, 21–28.

Stepišnik, U., Grlj, A., Radoš, D., Žebre, M. 2016. Geomorphology of Blidinje, Dinaric Alps (Bosnia and Herzegovina). Journal of Maps 12, S1, 163–171. http://dx.doi.org/10.1080/17445647.2016.1187209

Stepišnik, U., Ferk, M., Kodelja, B., Medenjak, G., Mihevc, A., Natek, K., Žebre, M. 2009. Glaciokarst of western Orjen, Montenegro. Cave and karst science: the transactions of the British Cave Research Association 36, 1, 21–28.

Stone, J.O., Allan, G.L., Fifield, L.K., Cresswell, R.G. 1996. Cosmogenic chlorine–36 from calcium spallation. Geochimica et Cosmochimica Acta 60, 679–692. http://dx.doi.org/10.1016/0016-7037(95)00429-7

Styllas, M.N., Schimmelpfennig, I., Benedetti, L., Ghilardi, M., Aumaître, G., Bourlès, D., Keddadouche, K. 2018. Late–glacial and Holocene history of the northeast

Mediterranean mountain glaciers – New insights from in situ–produced ^{36}Cl–based cosmic ray exposure dating of paleo–glacier deposits on Mount Olympus, Greece. Quaternary Science Reviews 193, 244–265. https://doi.org/10.1016/j.quascirev.2018.06.020

Thomas, F., Godard, V., Bellier, O., Benedetti, L., Ollivier, V., Rizza, M., Guillou, V., Hollender, F., Aumaître, G., Bourlès, D.L., Keddadouche, K. 2018. Limited influence of climatic gradients on the denudation of a Mediterranean carbonate landscape. Geomorphology 316, 44–58. https://doi.org/10.1016/J.GEOMORPH.2018.04.014

Vojnogeografski institut 1969. Atlas klime Socijalističke Federativne Republike Jugoslavije.

Woodward, J.C., Macklin, M.G., Smith, G.R. 2004. Pleistocene glaciation in the mountains of Greece. In: Ehlers, J. & Gibbard, P.L. (eds.) Quaternary Glaciations—Extent and Chronology. Part I: Europe. Elsevier, Amsterdam, 155–173.

Žebre, M., Sarıkaya, M.A., Stepišnik, U., Yıldırım, C., Çiner, A. 2019. First ^{36}Cl cosmogenic moraine geochronology of the Dinaric mountain karst: Velež and Crvanj Mountains of Bosnia and Herzegovina. Quaternary Science Reviews 208, 54–75.

Žebre, M., Stepišnik, U. 2015a. Glaciokarst geomorphology of the Northern Dinaric Alps: Snežnik (Slovenia) and Gorski Kotar (Croatia). Journal of Maps, 1–9. https://doi.org/10.1080/17445647.2015.1095133

Žebre, M., Stepišnik, U. 2015b. Glaciokarst landforms and processes of the southern Dinaric Alps. Earth Surf. Process. Landforms 40, 1493–1505. https://doi.org/10.1002/esp.3731

Žebre, M., Stepišnik, U., Colucci, R. R., Forte, E., Monegato, G. 2016. Evolution of a karst polje influenced by glaciation: the Gomance piedmont polje (northern Dinaric Alps). Geomorphology 257, 143–154.

Zech, J., Terrizzano, C., García–Morabito, E., Veit, H., Zech, R. 2017. Timing and extent of

late pleistocene glaciation in the arid central Andes of Argentina and Chile (22–41_S). Geographical Research Letters 43, 697–718.

Zech, R., Glaser, B., Sosin, P., Kubik, P.W, Zech, W. 2005. Evidence for long–lasting landform surface instability on hummocky moraines in the Pamir Mountains (Tajikistan) from ^{10}Be surface exposure dating. Earth and Planetary Science Letters 237, 453– 461.

Figures

Figure 1: a) Study area location map in Bosnia and Herzegovina (BIH); b) Glacial deposits of Svinjača (Figure 2) and Glavice (Figure 4) are located within the Blidinje Polje. Location of glacial deposits after Stepišnik et al. (2016) and Sofilj and Živanović (1979).

Figure 2: Geomorphological map of glacial landforms on the Svinjača Mountain. Samples for ^{36}Cl cosmogenic nuclide dating were collected from the hummocky (SV16–01 thru 05) and left lateral (SV16–06, 07 and 08) moraines. The samples ID`s along with the ages (ka) corrected for 40 mm ka^{-1} of erosion were presented.

Figure 3: Svinjača area moraines; a) Typical view of the hummocky moraines (HM) with knob and kettle topography. Blidinje Lake is seen at the horizon (photo looking to northeast), b) left lateral (LLM) and hummocky moraines (HM) (photo looking to W), c) exit of the glacial and the left lateral moraine (LLM) (photo looking to E), d) cross section of the lateral moraine with unsorted and unstratified limestone boulders floating in a sandy matrix. White and red arrows indicate palaeo–ice flow directions. Houses (a, b, c) and person (d) for scale.

Figure 4: Geomorphological map of glacial landforms on the Glavice Mountain. Samples for ^{36}Cl cosmogenic nuclide dating were collected from the terminal moraine (GL16–01 thru 04). The samples ID`s along with the ages (ka) corrected for 40 mm ka^{-1} of erosion were presented.

Figure 5: Glavice terminal moraine pictures; a) a typical amphitheater shaped terminal moraine (overgrown by forest) covering part of the Blidinje Polje (view from northeast towards southwest), b) the frontal view of terminal moraine with Stećak –monumental Medieval (12th – 15th Century) tombstones found scattered across BIH, inscribed as

UNESCO's World Heritage Site since 2016– at the foreground, c) close–up view of the terminal moraines.

Figure 6: Photos of the sampled boulders from the Svinjača hummocky (SV16–01 to SV16–05) and lateral moraines (SV16–06 to SV16–08).

Figure 7: Photos of the sampled boulders from the Glavice terminal moraine complex.

Figure 8: Cosmogenic ^{36}Cl ages of the boulders from (a) hummocky moraines and left–lateral (LLM) moraines of Svinjača and (b) terminal moraines of Glavice areas. Upper panels show the individual sample ages with 1–sigma uncertainties, and the lower panels show the probably density functions (PDF) of the samples. Oldest age of the moraines (indicated by thick black PDF curves) from both data sets were shown and assigned to the age of the landforms.

Figure 9: (a) All locations in the Balkan Peninsula where moraines/outwash have been dated so far. Base layer of mountain belts is from https://ilias.unibe.ch/goto.php?target=file_1049915, based on the mountain definition by Kapos et al. (2000). Bathymetric data is from the European Marine Observation and Data Network (http://www.emodnet.eu/), while the sea level data for LGM and Younger Dryas is from Lambeck et al. (2011).

Tables

Table 1: Sample locations, attributes and local corrections to production rates.

Table 2: Geochemical analytical data.

Table 3: Meteorological data obtained from measurements at Nevesinje station (~40 km southeast of the study area) used to estimate the snow depth on top of the sampled boulders.

Table 4: Cosmogenic ^{36}Cl inventories, production rates, ages of boulders considering 0 mm ka^{-1} and 40 mm ka^{-1} erosion rates and ages of glacial landforms in the Svinjača and Glavice areas.

Table 5: A list of different dating methods applied to glacial landforms in the Balkan Peninsula (modified from Žebre et al., 2019). Note that calculations of ^{36}Cl cosmogenic exposure ages from Mount Chelmos and Mount Olympus are based on the production rates from Stone et al. (1996) and Schimmelpfennig et al. (2011), respectively. For comparison, two boulder–ages from Mount Chelmos (CH10 (11.03 ± 0.9 ka), CH11 (8.76 ± 0.70 ka)) (Pope et al., 2015) and two boulder–ages from Mount Olympus (TZ03 (12.44 ± 1.07 ka), MK12 (12.37 ± 1.07 ka)) (Styllas et al., 2018) were recalculated using the production rates of Marrero et al. (2016b). The two ages from Mount Olympus were also corrected for snow and erosion, using the same values as in the paper of Styllas et al. (2018). The recalculated ages are 13–14% younger for Mount Chelmos and 23–24% younger for Mount Olympus with respect to the published ages. ^{14}C ages from Sneznik were recalculated according to the IntCal13 calibration (Reimer et al., 2013). Recalculated ages are marked with asterisk.

Supplementary Table S1: Supplementary laboratory and AMS data.

Table 1

	Sample ID	Latitude (WGS84) °N (DD)	Longitude (WGS84) °E (DD)	Elevation* (m)	Boulder dimensions (LxWxH) (m)	Sample thickness (cm)	Topography correction factor
1	SV16-01	43.5929	17.4654	1252	3x1.5x1	3	0.9964
2	SV16-02	43.5943	17.4693	1257	1.5x1x0.8	2	0.9958
3	SV16-03	43.5957	17.4727	1240	3x2x1.2	2	0.9982
4	SV16-04	43.5922	17.4653	1252	1x2x1	3	0.9964
5	SV16-05	43.5898	17.4658	1242	1.3x1x0.8	2	0.9843
6	SV16-06	43.5874	17.4745	1302	1x1x0.5	4	0.9771
7	SV16-07	43.5875	17.4741	1307	1.5x1x0.6	3	0.9771
8	SV16-08	43.5877	17.4733	1298	0.6x1x0.4	3	0.9771
9	GL16-01	43.6321	17.5315	1285	1x1x0.4	2	0.9896
10	GL16-02	43.6363	17.5299	1271	1.5x1.5x0.8	4	0.9963
11	GL16-03	43.6480	17.5374	1278	0.5x0.4x0.25	4	0.9982
12	GL16-04	43.6366	17.5302	1268	2.5x2x1	3	0.9927

Table 2

Click here to access/download;Table;Table 2_ChemData_Blidinje.xlsx

Table 2

		Major elements											Trace elements				
	Sample ID	Al_2O_3 (wt. %)	CaO (wt. %)	Fe_2O_3 (wt. %)	K_2O (wt. %)	MgO (wt. %)	MnO (wt. %)	Na_2O (wt. %)	P_2O_5 (wt. %)	SiO_2 (wt. %)	TiO_2 (wt. %)	CO_2 (LOI) (wt. %)	Sm (ppm)	Gd (ppm)	U (ppm)	Th (ppm)	Cl (ppm)
1	SV16-01	0.18	54.45	0.15	0.03	0.56	0.01	0.03	0.04	0.56	0.01	43.90	0.11	0.16	2.40	0.20	13.6 ± 1.3
2	SV16-02	0.07	55.12	0.08	0.01	0.48	0.02	0.01	0.04	0.39	0.01	43.70	0.13	0.16	0.80	0.20	14.0 ± 1.3
3	SV16-03	0.05	54.80	0.09	0.01	0.72	0.02	0.01	0.10	0.50	0.01	43.60	0.13	0.11	0.60	0.20	11.7 ± 1.1
4	SV16-04	0.05	55.34	0.07	0.01	0.44	0.01	0.01	0.05	0.36	0.01	43.60	0.11	0.18	0.80	0.20	9.1 ± 0.8
5	SV16-05	0.12	54.92	0.07	0.01	0.52	0.01	0.02	0.01	0.48	0.01	43.70	0.05	0.05	2.10	0.20	13.2 ± 1.2
6	SV16-06	0.06	54.98	0.06	0.01	0.67	0.01	0.01	0.01	0.26	0.01	43.90	0.05	0.06	1.60	0.20	18.5 ± 1.7
7	SV16-07	0.03	55.29	0.06	0.01	0.58	0.01	0.02	0.01	0.15	0.01	43.80	0.05	0.05	1.80	0.20	16.4 ± 1.5
8	SV16-08	0.01	55.32	0.06	0.01	0.51	0.01	0.01	0.01	0.21	0.01	43.80	0.05	0.05	2.10	0.20	5.6 ± 0.5
9	GL16-01	0.02	54.85	0.06	0.01	0.88	0.01	0.03	0.01	0.18	0.01	43.90	0.05	0.05	8.30	0.20	39.0 ± 3.5
10	GL16-02	0.03	55.28	0.07	0.01	0.53	0.01	0.02	0.01	0.24	0.01	43.80	0.05	0.05	2.80	0.20	56.6 ± 5.1
11	GL16-03	0.02	55.30	0.06	0.01	0.58	0.01	0.01	0.01	0.16	0.01	43.80	0.07	0.09	0.50	0.20	25.3 ± 2.3
12	GL16-04	0.04	54.81	0.04	0.01	0.71	0.01	0.02	0.01	0.40	0.01	43.90	0.05	0.05	5.10	0.20	28.7 ± 2.6

Table 3

Click here to access/download;Table;Table 3_SnowData_Blidinje.xlsx

Months	I	II	III
Temperature, ^{o}C, at Nevesinje station (@900 m asl)	-0.9	0.5	3.5
Precipitation, mm, at Nevesinje station	171	169	165
Snow depth, cm, measured at Nevesinje station	117	70	53
Temperature @1270 m asl using 6.5 ^{o}C km^{-1} temp. lapse rate	-3.3	-1.9	1.1
Minimum snow water equivalent, mm (=prec, if temp<0)	171	169	0
Minimum snow depth, cm (using the 10:1 snow depth ratio)	171	169	0
Our snowpack estimates on top of boulders (aver. boulder height 70 cm)	**100**	**100**	**50**

IV	V	VI	VII	VIII	IX	X	XI	XII
7.5	12.3	15.5	18.0	17.8	14.2	9.7	4.8	0.5
162	119	97	65	85	116	178	242	225
34	4	0	0	0	0	10	30	65
5.1	9.9	13	16	15	12	7.3	2.4	-1.9
0	0	0	0	0	0	0	0	225
0	0	0	0	0	0	0	0	225
25	**0**	**0**	**0**	**0**	**0**	**0**	**25**	**100**

Table 4

	Sample ID	Landform	^{36}Cl (measured)	Surface Exposure Ages: Erosion corrected (0 mm ka^{-1})	Surface Exposure Ages: Erosion corrected (40 mm ka^{-1})	Landform Age
			(10^4 atoms g^{-1} rock)	(ka)	(ka)	(ka)
Svinjača						
1	SV16-01	Hummocky Moraine	49.28 ± 1.63	8.7 ± 0.8	12.2 ± 1.4	
2	SV16-02	Hummocky Moraine	72.19 ± 2.44	12.7 ± 1.1	**22.7 ± 3.8**	
3	SV16-03	Hummocky Moraine	59.22 ± 2.21	10.6 ± 1.0	16.6 ± 2.4	**22.7 ± 3.8**
4	SV16-04	Hummocky Moraine	58.31 ± 2.28	10.4 ± 0.9	16.4 ± 2.4	
5	SV16-05	Hummocky Moraine	69.78 ± 2.23	13.0 ± 1.0	22.5 ± 3.8	
6	SV16-06	Lateral Moraine	46.90 ± 1.78	8.0 ± 0.7	10.6 ± 1.3	
7	SV16-07	Lateral Moraine	49.82 ± 1.73	8.4 ± 0.7	11.5 ± 1.5	**13.2 ± 1.8**
8	SV16-08	Lateral Moraine	50.76 ± 2.18	8.9 ± 0.8	**13.2 ± 1.8**	
Glavice						
9	GL16-01	Terminal Moraine	50.98 ± 1.86	8.0 ± 0.6	9.7 ± 1.1	
10	GL16-02	Terminal Moraine	47.46 ± 5.91	7.0 ± 1.0	8.2 ± 1.5	**13.5 ± 1.8**
11	GL16-03	Terminal Moraine	43.47 ± 1.65	7.3 ± 0.6	9.0 ± 1.0	
12	GL16-04	Terminal Moraine	58.80 ± 1.91	9.9 ± 0.9	**13.5 ± 1.8**	

Table 5

Mountain	Dating method	Age
Snežnik (Croatia)	14C	LGM (18.7 ±1.0 cal kyr BP*)
Pindus (Greece)	U-series	MIS 12 (>350-71 ka), MIS 6 (131.3-80.5 ka)
Šar Planina (FYROM)	10Be cosmogenic exposure dating	LGM (19.4 ± 3.2 ka to 12.4 ± 1.7 ka), Younger Dryas (14.7 ± 2.1 to 11.9 ± 1.7 ka)
Orjen (Montenegro)	U-series	MIS 12 (>350-324.0 ka), MIS 6 (124.6-102.4 ka), MIS 5d-2 (17.3-12.5 ka), Younger Dryas (9.6-8.0 ka)
Central Montenegro	U-series	MIS 12 (>350 ka; 396.6-38.8 ka), MIS 8 or 10 (231.9-58.8 ka), MIS 6 (120.2-88.1 ka) MIS 2 (13.4 ka), Younger Dryas (10.9-2.2 ka)
Velebit mountain, Velebit channel (Croatia)	U-series	MIS 12-6 (>350-61.5 ka)
Rila (Bulgaria)	10Be cosmogenic exposure dating	LGM (23.5-14.4 ka)
Chelmos (Greece)	**36Cl cosmogenic exposure dating**	MIS 3 (39.9 ± 3.0 ka to 30.4 ± 2.2 ka), LGM (22.9 ±1.6 ka to 21.2 ± 1.6 ka), Younger Dryas (12.6 ± 0.9 ka to 10.2 ± 0.7 ka)
Galičica (FYROM)	**36Cl cosmogenic exposure dating**	Younger Dryas (12.8 ± 1.4 ka to 11.3 ± 1.3)
Pelister (FYROM)	10Be cosmogenic exposure dating	Oldest Dryas (15.56 ± 0.85 to 15.03 ± 0.85)
Olympus (Greece)	**36Cl cosmogenic exposure dating**	Lateglacial (3 phases: 15.5 ± 2.0 ka, 13.5 ± 2.0 ka, 12.5 ± 1.5 ka), Holocene (3 phases: 9.6 ± 1.1 ka, 2.5 ± 0.3 ka, 0.64 ± 0.08ka)
Velež and Crvanj (Bosnia and Herzegovina)	**36Cl cosmogenic exposure dating**	Oldest Dryas (14.9 ± 1.1 ka) Younger Dryas j (11.9 ± 0.9 ka)

Erosion rate	Number of samples	Reference
/	1 (animal bone in outwash fan)	Marjanac et al., 2001
/	28 from at least 11 landforms (calcite cement from moraines and alluvial deposits)	Hughes et al., 2006; Woodward et al., 2004
10 mm/ka	8 from at least 6 landforms (moraine boulders)	Kuhlemann et al., 2009
/	12 from 7 landforms (calcite cement from moraines)	Hughes et al., 2010
/	19 from 11 landforms (calcite cement from moraines)	Hughes et al., 2011
/	9 from at least 6 landforms (calcite cement from moraines, paleocaverns, former ice wedges)	Marjanac, 2012
0 mm/ka	10 from at least 6 landforms (moraine boulders)	Kuhlemann et al., 2013
0 mm/ka	7 from 4 different landforms (moraine boulders)	Pope et al., 2015
5 mm/ka	5 from 1 landform (moraine boulders)	Gromig et al., 2018
0 mm/ka	3 from 1 landform (moraine boulders)	Ribolini et al., 2018
0 mm/ka	20 from 11 landforms (moraine boulders, bedrock)	Styllas et al., 2018
40 mm/ka	20 from 4 landforms (moraine boulders)	Žebre et al., 2019

Figure 1

Click here to access/download;Figure;1. Figure_StudyArea.jpg

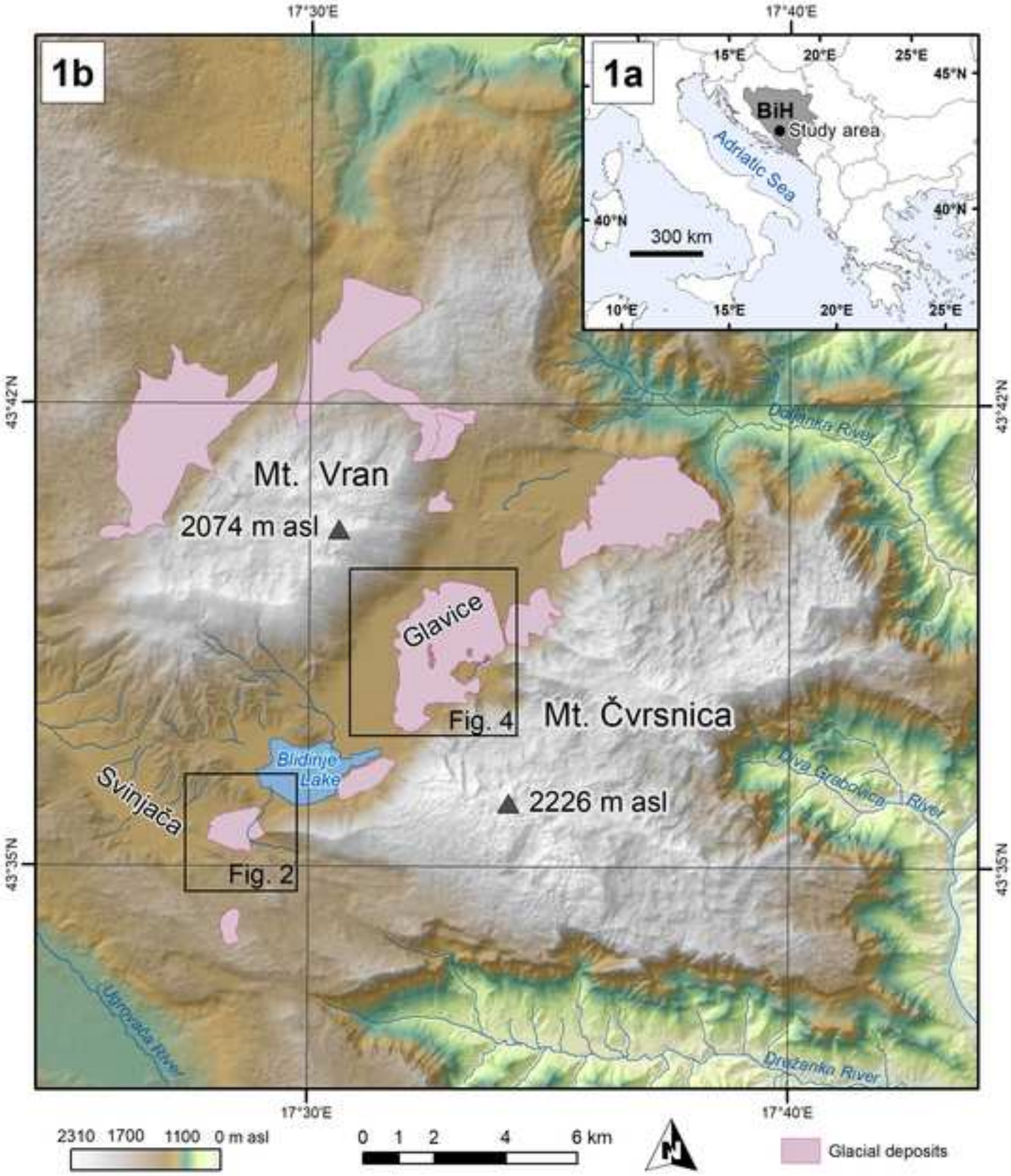

Figure 2

Click here to access/download;Figure;2. Figure_Svinjaca.jpg

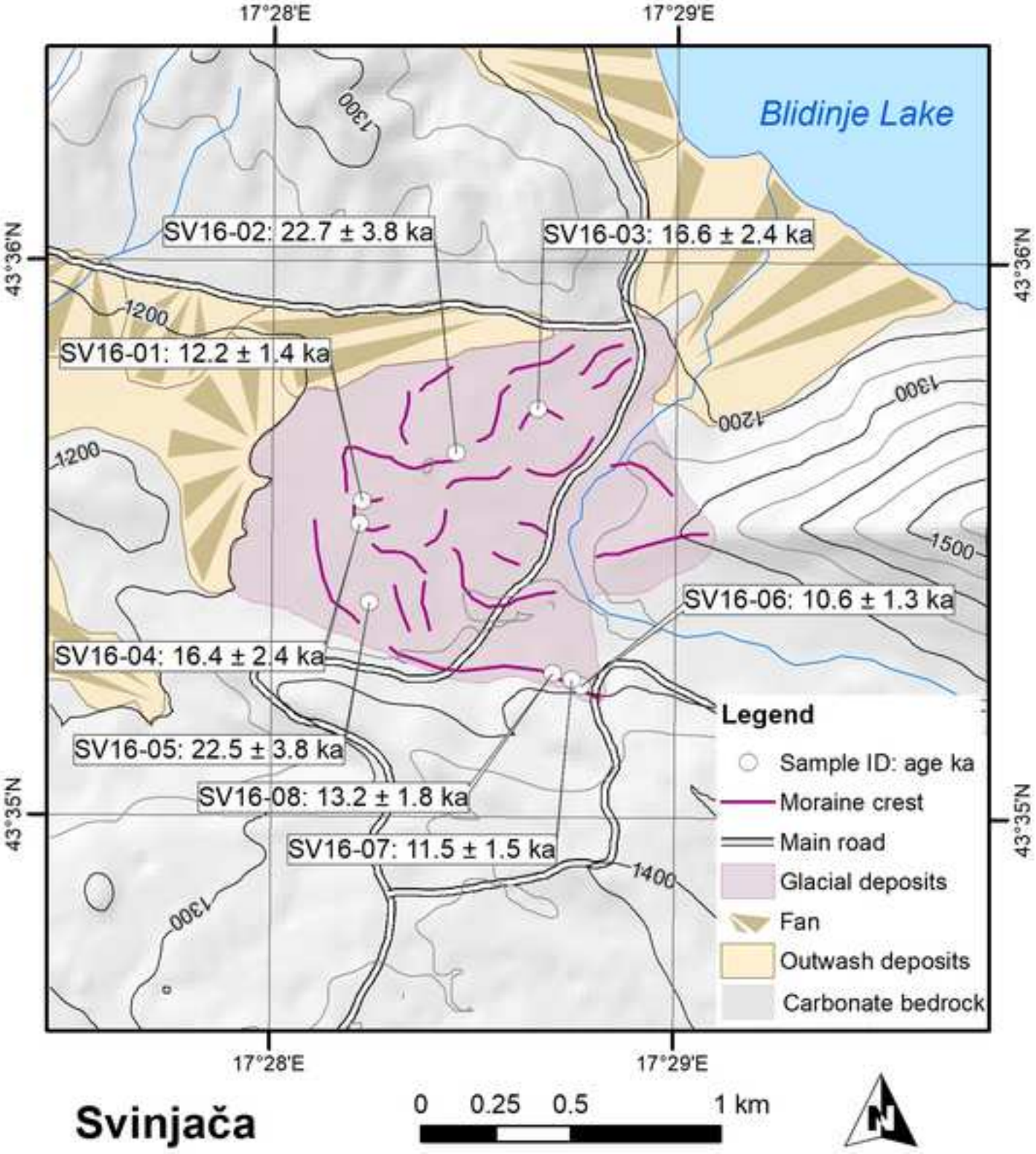

Figure 3

Click here to access/download;Figure;3. Svinjaca HM & LLM.tif

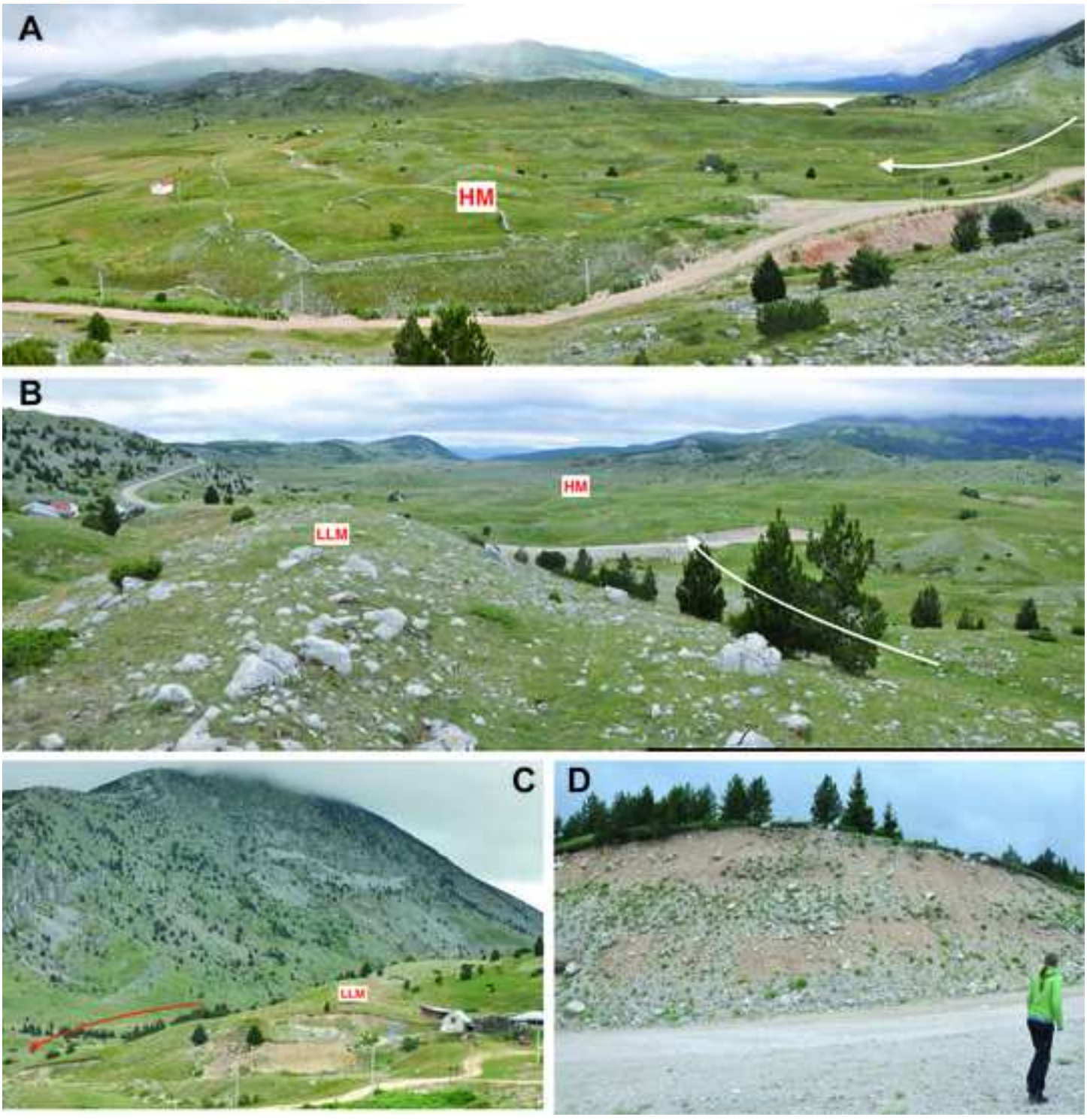

Figure 4

Click here to access/download;Figure;4. Figure_Glavice.jpg

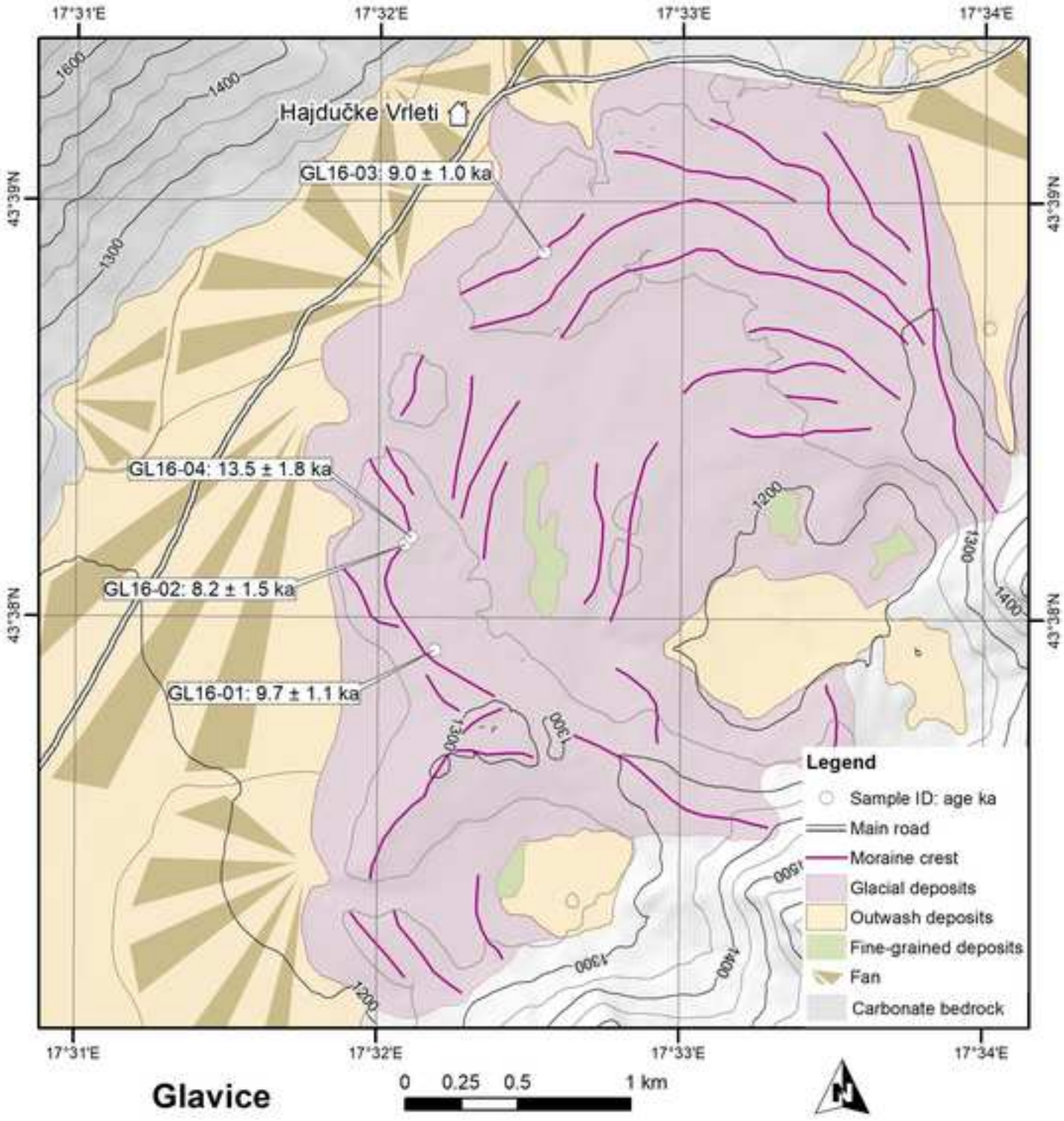

Figure 5

Click here to access/download;Figure;5. Glavice.tif

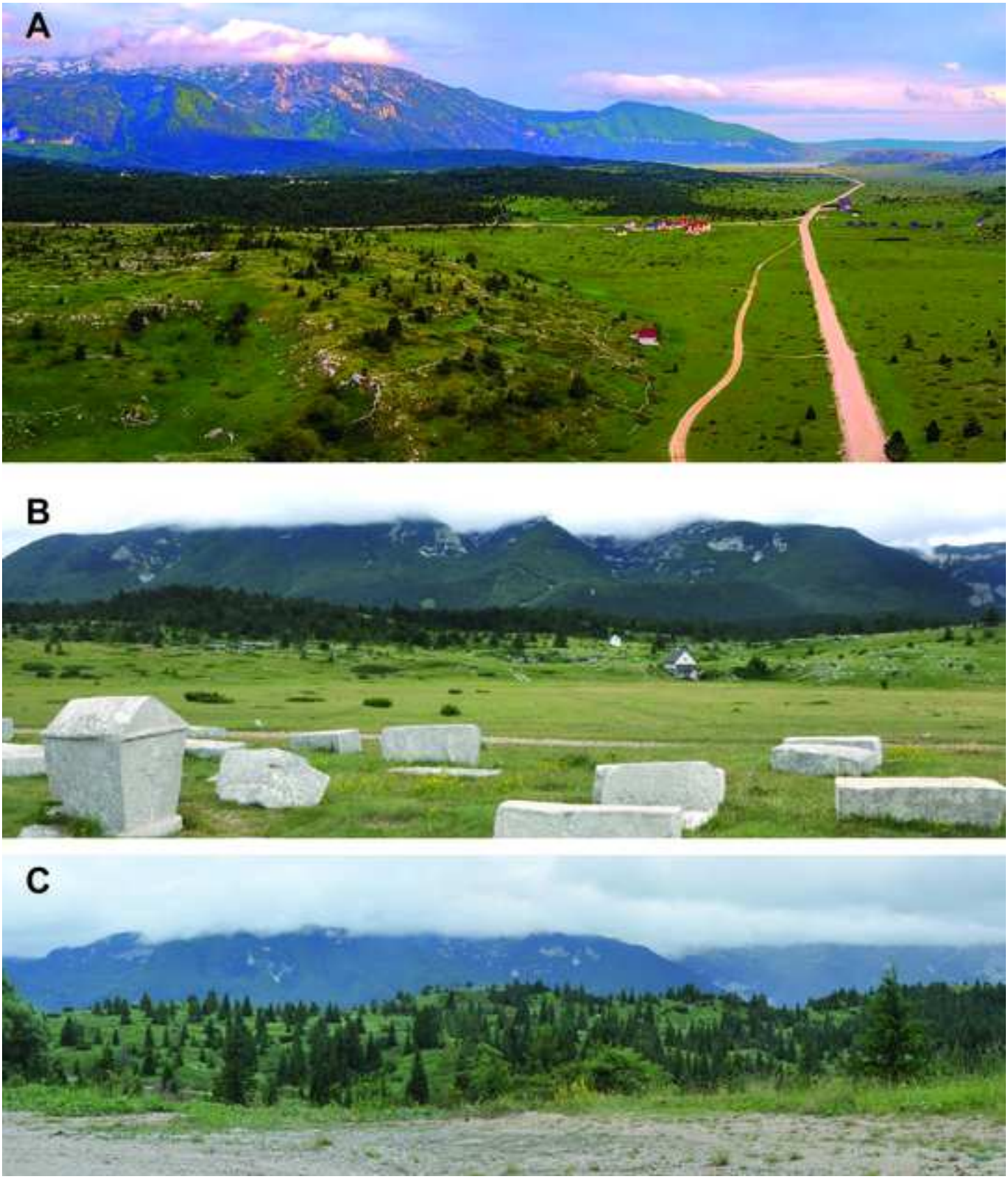

Figure 6

Click here to access/download;Figure;6. Svinjica samples.tif

Figure 7

Click here to access/download;Figure;7. GLavice pictures.tif

Figure 8

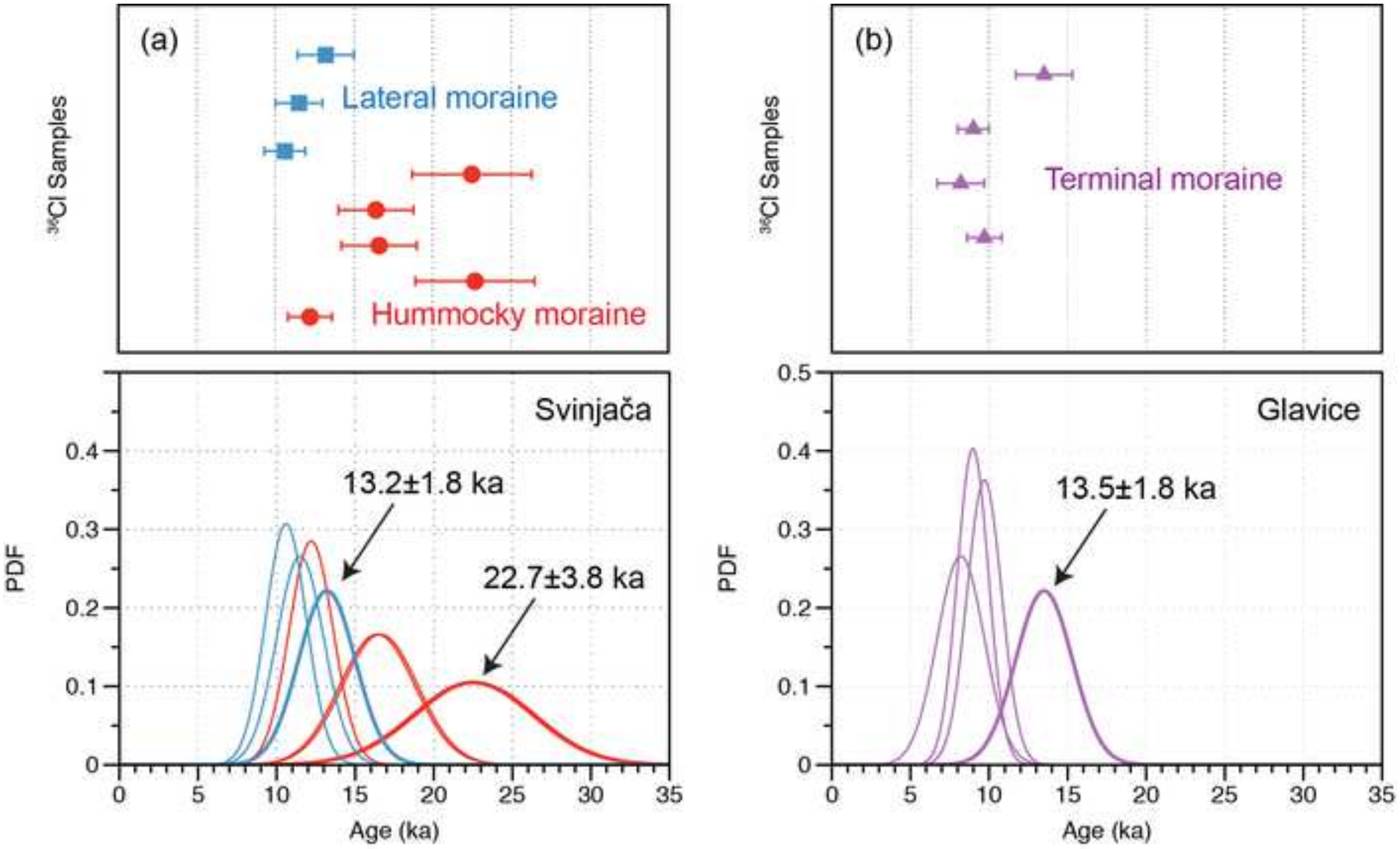

Figure 9

Click here to access/download;Figure;9. Balkan ages.jpg

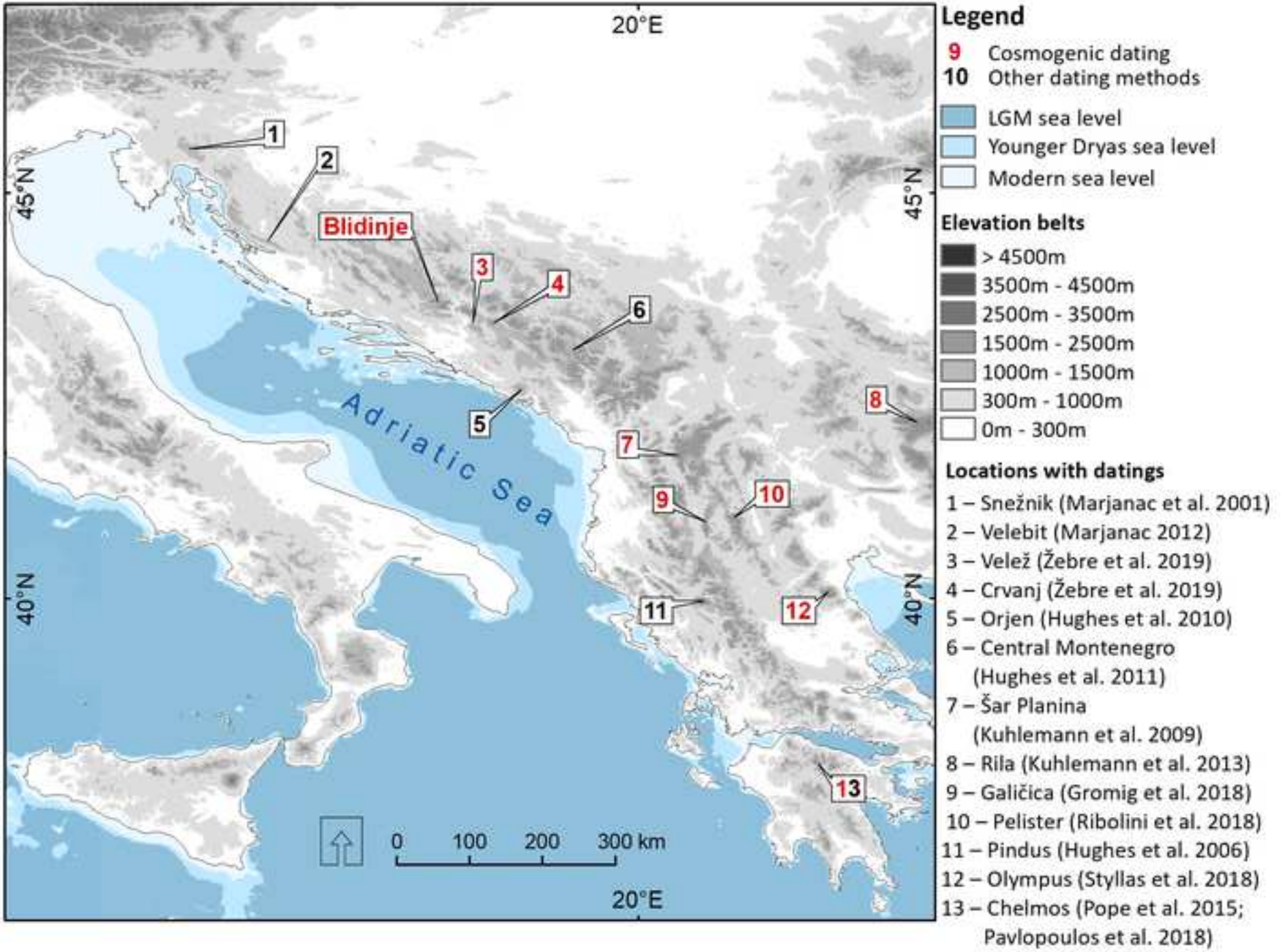

Table S1-Sup Material

Click here to access/download

Supplementary Material

TableS1_supplemantaryAMSdata.xlsx